

**LAPPEENRANTA UNIVERSITY OF TECHNOLOGY**

LUT School of Engineering Sciences

Master's Degree Programme in Chemical and Process Engineering

Master's Thesis

Iakupov Dmitrii

**Phenolic resin processing unit development and energy optimization in phenol and acetone production**

Examiners: Professor Tuomas Koiranen

Docent Arto Laari

Supervisors: Professor Tuomas Koiranen

Docent Arto Laari

Tech.Lic. Esko Lahdenperä

## **Abstract**

Lappeenranta University of Technology

School of Engineering Science

Degree Program in Chemical and Process Engineering

Dmitrii Iakupov

### **Phenolic resin processing unit development and energy optimization in phenol and acetone production**

Master's Thesis

2019

Examiners: Professor Tuomas Koiranen  
Docent Arto Laari

Supervisors: Professor Tuomas Koiranen  
Docent Arto Laari  
Tech.Lic. Esko Lahdenperä

65 pages, 16 figures, 24 tables, 2 appendices

Keywords: phenolic resin, waste reduction, feasibility analysis, energy conservation, process design

Phenol is a substance extensively used in the chemical industry. The fact that demand in phenol has been permanently increasing requires new efficient and sustainable solutions for its production. The cumene method of phenol production remains predominant in the industry, however, it poses the challenge of phenolic resin processing, which is the hazardous waste product formed in the process. The main goal of this Master's thesis was to develop the equipment and technology for phenolic resin processing unit used at phenol production by cumene process. It was especially important to ensure profitability of the technology and sustainability of the unit, as well as to reduce adverse environmental impact from production. The literature review was done to find the most economically efficient flowsheet which would allow to reduce adverse environmental impact as well. Apart from that, the project economic evaluation was made. Aspen Plus and Aspen Hysys were used to simulate phenolic resin processing unit and find optimal parameters of distillation columns. Aspen Energy Analyzer was used to make pinch analysis based on the heat flows obtained by simulation in Aspen Hysys. As a result, the project utility costs were reduced with the help of created heat exchanger network, and 310 kg/h of commercial cumene and 1000 kg/h of alpha-methylstyrene were obtained, with commercial phenol yield increase by 500 kg/h, providing that a typical phenolic resin composition was used, and 200000 t/year of

phenol and 125000 t/year of acetone were taken as typical capacity for phenol production. The results obtained in this Master's thesis allowed to consider the designed phenolic resin processing unit suitable for phenol and acetone production plants by cumene method, with its implementation encouraging profitability and sustainability of production with economic potential of 7.36 M€/year.

## **Acknowledgements**

This Master's thesis was done at LUTs Department of Chemical Engineering in Lappeenranta in the period between February and June in 2019. I want to express my gratitude to Professor Tuomas Koiranen for his approval of the Master's thesis topic that I proposed, his managing and constructive ideas which increased the level of work. I also want to thank Tech.Lic. Esko Lahdenperä for providing invaluable help with the work and Docent Arto Laari for his indispensable advice concerning writing and process design.

I want to express gratitude to my family for their unfailing support.

Lappeenranta, Finland 24.06.2019

## List of contents

Abstract.....	II
Acknowledgements .....	IV
List of contents .....	V
List of figures .....	VII
List of tables .....	VIII
List of abbreviations .....	IX
List of symbols .....	IX
Introduction .....	XII
LITERATURE REVIEW .....	1
1 Phenol production products characteristics.....	1
2 Phenol production methods.....	5
2.1 Cumene process.....	5
2.3 Toluene and benzoic acid process .....	9
2.4 Modern alternatives of phenol production .....	10
2.4.1 Direct oxidation of benzene to phenol.....	12
2.4.2 Oxidation of benzene by $N_2O$ to phenol.....	12
2.4.3 Joint production of phenol and methylethylketone.....	16
2.4.4 Conclusion on modern alternative processes.....	18
3 Phenolic resin processing .....	19
3.1 Phenolic resin processing methods.....	19
3.2 Thermal cracking of phenolic resin.....	20
EXPERIMENTAL PART .....	22
4 Phenolic processing unit process design.....	22
5 Simulations.....	23
5.1 Simulation of phenol-acetone distillation with Aspen Hysys .....	23
5.2 Phenol-acetone distillation process description.....	23
5.3 Reactor simulation: Aspen Plus.....	26
5.4 Simulation of decomposed phenolic resin distillation: Aspen Hysys .....	29
6 Pinch analysis.....	35
7 Equipment sizing.....	37
7.1 Distillation columns sizing .....	37
7.2 Reactor sizing .....	37
7.3 Heat exchangers sizing .....	38
7.4 Pumps sizing.....	39
8 Economic evaluation.....	40
8.1 Capital costs.....	40

8.2	Operational costs .....	43
8.3	Economic potential .....	43
	Conclusion .....	45
	REFERENCES .....	47
	APPENDICES .....	55
	Appendix I Calculation of valve tray .....	55
	Appendix II Calculation of vessel mass .....	61

**List of figures**

- Figure 1 Phenol production by cumene process (McKetta Jr 1990)
- Figure 2 Cumene oxidation to hydroperoxide (Matar, Hatch 2001)
- Figure 3 Obtaining phenol by CHP cleavage with acidic medium (Matar, Hatch 2001)
- Figure 4 Typical phenol production from cumene. a) Oxidation reactor for cumene; b) Waste gas purification; c) Gas separator; d) Concentration; e) Reactor for cleavage reaction; f) Catalyst separation; g) Column for acetone separation; g) Column for cumene separation; i) Column for phenol separation; j) Cracking; k) Hydrogenation (McKetta Jr 1990)
- Figure 5 Toluene and benzoic acid production of phenol (McKetta Jr 1990)
- Figure 6 Block diagram of toluene and benzoic acid production of phenol (McKetta Jr 1990)
- Figure 7 Reactions of joint production of phenol and methylethylketone (Zakoshansky 2009)
- Figure 8 Phenol production by cumene process with phenolic processing unit.
- Figure 9 Typical diagram of phenol and acetone distillation at phenol production by cumene method (Romanova, Leontiev 2017)
- Figure 10 Simulation of phenol and acetone distillation in Aspen Hysys
- Figure 11 Reactor simulation in Aspen Plus
- Figure 12 Diagram of phenolic resin processing unit
- Figure 13 Simulation of phenolic resin processing unit distillation
- Figure 14 Diagram for choosing the number of stages and reflux ratio
- Figure 15 Inlet data for pinch analysis. H – hot stream, C – cold stream, D – column
- Figure 16 Heat integration system

**List of tables**

Table I	Phenol product specifications (Altivia 2015)
Table II	Acetone product specifications (Colonial 2019)
Table III	AMS product specifications (Advansix 2018)
Table IV	Cumene product specifications (Dow 2013)
Table V	Phenol production product prices
Table VI	Typical composition of phenolic resin (Zakoshansky 2009)
Table VII	Distillation column parameters for phenol and acetone separation
Table VIII	Mass balance for phenol and acetone separation
Table IX	Energy balance for phenol and acetone separation
Table X	Phenolic resin decomposition with thermal cracking (Vol'-Epshtein, Gagarin 1973, Zakoshansky 2007).
Table XI	Thermal cracking reactor mass balance
Table XII	Boiling points of decomposed phenolic resin components (Weast, Astle et al. 1988)
Table XIII	Distillation column parameters of phenolic resin processing unit
Table XIV	Mass balance for phenolic resin processing unit
Table XV	Energy balance for phenolic resin processing unit
Table XVI	Utility streams with and without HEN
Table XVII	Distillation column sizing parameters
Table XVIII	Heat exchangers for system with and without HEN
Table XIX	Calculated pump parameters
Table XX	Prices for system with and without HEN
Table XXI	Project capital costs
Table XXII	Project operational costs
Table XXIII	Project revenue
Table XXIV	Parameters for tray calculation for column D-8

## List of abbreviations

AMS	alpha-methylstyrene
CEPCI	engineering plant cost index
CHP	cumene hydroperoxide
CPI	consumer price index
EAC	equivalent annual costs
HEN	heat exchanger network
IRR	internal rate of return
MER	maximum energy recovery

## List of symbols

$A_1$	first calculated coefficient	[-]
$A_2$	second calculated coefficient	[-]
$A_3$	third calculated coefficient	[-]
$a$	first cost constant	[-]
$B_1$	load factor	[-]
$B_3$	valve opening coefficient	[-]
$b$	second cost constant	[-]
$C_p$	calculated equipment price	[\$]
$C_{p2010}$	calculated equipment price for the year 2010	[\$]
$C_{p2018}$	calculated equipment price for the year 2018	[\$]
$C_{pinst}$	installed equipment price	[\$]
$c$	allowance	[mm]
$c_0$	standard rolled thickness allowance	[mm]
$c_1$	corrosion allowance	[mm]
$c_2$	negative tolerance allowance	[mm]
$D$	tray diameter	[m]
$D_c$	calculated tray diameter	[m]
$D_d$	vessel diameter	[mm]
$D_e$	vessel external diameter	[m]
$D_i$	vessel internal diameter	[m]
$e$	liquid entrainment between trays	[-]
$F$	steam load factor	$\left[ \frac{kg^{0,5}}{m^{0,5}s} \right]$

$F_{inst}$	installation factor	[-]
$F_{max}$	maximum steam load factor	$[\frac{kg^{0.5}}{m^{0.5}s}]$
$F_R$	reactor flow rate	[m <sup>3</sup> /h]
$f_3$	standard relative tray free cross-section	[%]
$f_5$	working relative tray free cross-section	[%]
$G$	steam load	[kg/s]
$G_V$	steam volume load	[m <sup>3</sup> /s]
$g$	gravitational acceleration	[m/s <sup>2</sup> ]
$H$	distance between trays	[m]
$H_C$	height of separational space	[m]
$H_v$	vessel height	[m]
$h_1$	backwater height above overflow edge	[m]
$h_2$	height of gas-liquid layer on tray	[m]
$h_5$	minimum bubbling depth	[m]
$h_6$	dynamic bubbling depth	[m]
$h_7$	overflow edge height	[m]
$h_9$	initial bubbling depth	[m]
$J$	corrosion ratio	[mm/year]
$K_1$	phase equilibrium coefficient	[-]
$K_2$	surface tension dependent coefficient	[-]
$K_3$	load reduction coefficient	[-]
$K_5$	foaming coefficient	[-]
$KL$	standard valve count	[-]
$L$	fluid load, kg/s	[kg/s]
$L_V$	fluid volume load	[m <sup>3</sup> /s]
$L_{V1}$	fluid load per unit tray density	[m/s]
$L_{V2}$	fluid load per unit of overflow edge perimeter length	[m <sup>2</sup> /s]
$l_2$	overflow edge perimeter	[m]
$n_t$	theoretical number of stages	[-]
$n_{real}$	number of real trays	[-]
$p$	pressure	[MPa]
$p_c$	calculated pressure	[MPa]
$p_h$	hydraulic pressure	[MPa]

$p_t$	test pressure	[MPa]
$p_{hr}$	hydraulic resistance	[Pa]
$q$	specific valve load	[Pa]
$S$	column free cross-section	[m <sup>2</sup> ]
$S_1$	column working relative free cross-section	[m <sup>2</sup> ]
$S_2$	overflow relative free cross-section	[%]
$s$	wall thickness	[mm]
$s_c$	calculated wall thickness	[mm]
$T$	residence time	[h]
$U$	fluid velocity in overflow	[m/s]
$U_p$	permissible fluid velocity in overflow	[m/s]
$u$	exponent for type of equipment	[-]
$V_R$	reactor vessel volume	[m <sup>3</sup> ]
$V_{vessel}$	volume of vessel steel	[m <sup>3</sup> ]
$W$	steam velocity	[m/s]
$W_k$	steam velocity in free cross-section of valves	[m/s]
$W_{kmin}$	minimum steam velocity in free cross-section of valves	[m/s]
$W_{kmax}$	maximum steam velocity in free cross-section of valves	[m/s]
$W_p$	permissible steam velocity in tray working cross-section	[m/s]
$W_{pc}$	permissible steam velocity in the column	[m/s]
$Y$	size parameter	[-]
$\beta$	airing factor	[-]
$\zeta_o$	open valve hydraulic resistance coefficient	[-]
$\zeta_h$	coefficient of hydraulic resistance technological valve gaps	[-]
$\eta_{valve}$	energy conversion efficiency for valve tray	[-]
$\rho$	density	[kg/m <sup>3</sup> ]
$\rho_L$	liquid density	[kg/m <sup>3</sup> ]
$\rho_V$	vapor density	[kg/m <sup>3</sup> ]
$\rho_{steel}$	steel density	[kg/m <sup>3</sup> ]
$\sigma$	surface tension	[mN/m]
$\sigma$	admissible stress for working temperature	[MPa]
$\sigma_{20}$	admissible stress for 20 °C	[MPa]
$\tau$	life span	[year]
$\varphi$	weld strength factor	[-]

## **Introduction**

Phenol is an organic compound extensively used in a wide range of industries from oil and gas to pharmaceuticals. However, as of the chemical industry, phenol is mainly applied in bisphenol A production, which is used to produce polycarbonates and epoxy resins. The industry needs hundreds of thousands of tons of phenol annually, with these amounts permanently increasing. Joint production of phenol and acetone by the cumene method has proved to be the most common technology applied (Borealis 2019). The cumene method of phenol production has phenolic resin as its main waste product which is usually burnt as fuel despite the useful products it contains. In view of this, the industry may benefit from phenolic resin, for example by extracting the phenolic fraction by additional rectification before it is burnt. Thermal cracking allows turning part of phenolic resin into products suitable for production and thus increases the yield of commercial products. Apart from that, with phenol being a hazardous substance, the advanced processing of phenolic resin would encourage more sustainable production and reduce environmental impact (Zárate, Aranguren et al. 2008).

Thus, the key objective of this Master`s thesis work was to develop the equipment and technology for phenolic resin processing unit used at phenol production by cumene process. Aspen Plus and Aspen Hysys were used to simulate phenolic resin processing unit and find optimal parameters of distillation columns. Aspen Energy Analyzer was used to make pinch analysis based on heat flows obtained by simulation in Aspen Hysys. The literature review was done to find the most economically efficient flowsheet which would allow to reduce the adverse environmental impact as well. Apart from that, the project economic evaluation was made.

## LITERATURE REVIEW

### 1 Phenol production products characteristics

Phenol is a crystalline substance with a specific odor, it is toxic and highly irritating. It is used in the production of bisphenol A, which is later used in polycarbonates and ethoxyline resin production. It is also used in the production of phenol-formaldehyde resins. By converting phenol by hydrogenation to cyclohexanol, synthetic fibers, nylon and kapron, are obtained. In refining phenol is used to remove resinous substances, sulfur compounds and various polycyclic aromatic hydrocarbons with short side chains from oil. It is also actively used in the pharmaceutical industry for the synthesis of medicines (aspirin, salol) and cosmetology (chemical peeling). Acetone is a mobile volatile colorless liquid with a sharp specific odor. It is used as a raw material in production of essential chemicals (acetic anhydride, ketene, isophorone, etc.). It is a strong solvent and is used in the manufacturing of varnishes, explosives, medicines and films (Wallace, Updated by Staff 2000, Borealis 2019). Alpha-methylstyrene (AMS) is a colorless liquid with a strong odor. It is used as a monomer to produce synthetic rubbers, latex and waterproof mastic. Liquid AMS and its fumes are highly irritative. Cumene is a flammable and colorless liquid used in phenol and acetone production by cumene method. It is converted into cumene hydroperoxide (CHP) in the process. Phenolic resin is a hazardous waste product formed in phenol and acetone production by cumene method (Weast, Astle et al. 1988). Specifications of the products mentioned above are given in Tables I-IV.

Table I Phenol product specifications (Altivia 2015)

Parameter	Specifications
Appearance (Molten State)	Clear water white liquid
Appearance (Solid State)	White crystalline mass
Color, APHA (Molten)	20 Max.
Purity, % wt	99.6 Min.
Water, % wt	0.1 Max.
Solidification Point, °C	40.6 Min.

Table II Acetone product specifications (Colonial 2019)

Parameter	Specifications
Appearance	Liquid with a characteristic odor
Color, APHA	10 Max.
Specific Gravity 20 °C	0.791-0.793
Purity, % wt	99.5 Min.
Water Content, % wt	0.5 Max.
Acidity, as Acetic Acid, % wt	0.002 Max.
Alkalinity, % wt	0.001 Max.
Non-volatile Matter, ppm wt	20 Max.

Table III AMS product specifications (Advansix 2018)

Parameter	Specifications
Appearance	Clear water white liquid
Color, APHA	20 Max.
Specific Gravity 15.5 °C	0.912-0.915
Specific Gravity 25 °C	0.903-0.908
Purity, % wt	99.3 Min.
Phenol Content, ppm wt	20 Max.
Inhibitor Content (p-TBC), ppm wt	10-20

Table IV Cumene product specifications (Dow 2013)

Parameter	Specifications
Appearance	Colorless liquid
Color, APHA	10 Max.
Purity, % wt	99.9 Min.
Benzene, ppm wt	35 Max.
Ethylbenzene, ppm wt	200 Max.
n-Propylbenzene, ppm wt	300 Max.
Butylbenzenes, ppm wt	200 Max.
Diisopropylbenzenes, ppm wt	15 Max.
Phenol, ppm wt	5 Max.
CHP, ppm wt	100 Max.

Average prices for products mentioned above are presented in Table V. They were converted to € (Transferwise 2019) and updated by using consumer price index (CPI) for the year 2018 (USIC 2019).

Table V Phenol production product prices

Product	Price, €/t	Reference
Phenol	970	(Marketsinsider 2019, Intratec 2019, ICIS 2016)
AMS	700	(ICIS 2010)
Cumene	1320	(Intratec 2019, ICIS 2012)

Composition of phenolic resin differs because of different technologies of phenol and acetone production. Typical composition of phenolic resin is described in Table VI.

Table VI Typical composition of phenolic resin (Zakoshansky 2009)

Component	Concentration, % mass
Ortho- and para- cumylphenol	40-50
AMS dimers	20-30
Acetophenone	10-20
Phenol	2-20
Dimethylphenylcarbinol	0.3-1
Polyalkylphenols and other products of deep condensation	10-30
Phenol sodium	0.1-2.5
Inorganic salts (Na <sub>2</sub> SO <sub>4</sub> mostly)	0.1-4
Cumene and AMS	0.3-3

The ratio of the components in phenolic resin depends on the selectivity of the stages of cumene oxidation and decomposition of CHP. More than 60 chemical combinations are found in phenolic resin, but only 20 of them have been identified (Knop, Pilato 2013). Composition of phenolic resin shows that there is an opportunity to turn some of its chemical combinations into products at certain process conditions or use them separately after purification. However, heavy components of this composition are unlikely to be used in further production as they have high boiling temperatures, high viscosity and low chilling point (Zakoshansky 2007).

## 2 Phenol production methods

Since the discovery of phenol, several methods of its industrial production have been discovered (Schmidt 2005, Rappoport 2004, Wallace, Updated by Staff 2000), namely:

- a) Benzene sulphonation and phenol production by benzene sulfonate thermal treatment in molten alkali hydroxide;
- b) Benzene chlorination and chlorobenzene alkaline hydrolysis;
- c) Benzene chlorination and chlorobenzene steam hydrolysis;
- d) Benzene alkylation with propane to cumene, oxidation of cumene to tert-hydroperoxide and subsequent cleavage to acetone and phenol;
- e) Toluene oxidation to benzoic acid and oxidizing decarboxylation to phenol;
- f) Cyclohexanol – cyclohexanone mixtures dehydrogenation.

However, the cumene process has proved to be the most effective method of phenol and acetone production. The toluene oxidation method is also important for the industry. Other processes have shown the lack of economic efficiency (Gera, Panahi et al. 2012).

### 2.1 Cumene process

The cumene process has acetone as its byproduct. Since acetone is also in demand in the market, it does not pose a problem for phenol production, and the cumene process, therefore, became widely spread. Today this method prevails in phenol production, and is the predominant method used at new plants. The cumene method was invented in 1942 by a group of Soviet chemists headed by P.G. Sergeev, and independently by Heinrich Hock in 1944. Many licensed processes based on the cumene process have been created since then.

The process includes the following stages (Luyben 2009):

- a) Production of cumene by alkylation of benzene with propylene;
- b) Oxidation of cumene to CHP with oxygen extracted from air;
- c) Decomposition of CHP to phenol and acetone.

A simplified block diagram of the cumene process can be found in Figure 1.

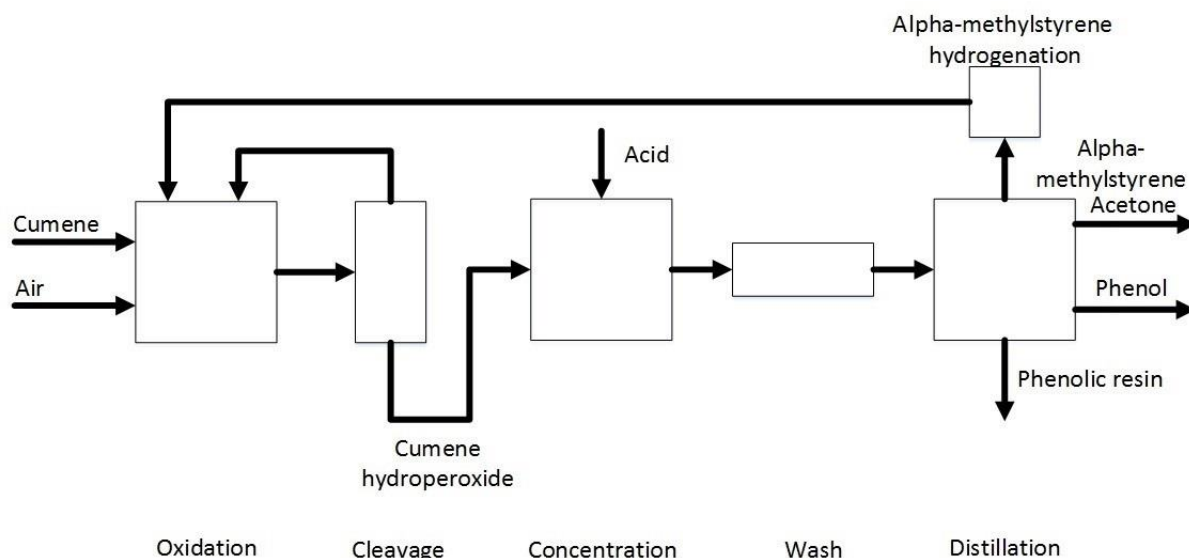


Figure 1 Phenol production by cumene process (McKetta Jr 1990)

Oxidation reaction that can be found in Figure 2 is carried out in bubble column reactor. The reactor is constructed from steel or stainless steel. The reactors that are more than 20 m high are connected in cascade to achieve the optimal distribution of residence time. Three or four oxidation reactors in series are usually used to achieve CHP by oxidation of cumene. Each of these reactors has about the same fractional conversion. The oxidation process is done at the temperature of 90-120 °C (Schmidt 2005).

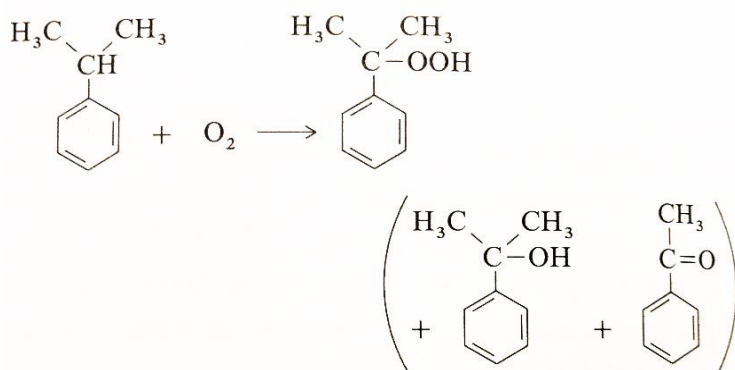


Figure 2 Cumene oxidation to hydroperoxide (Matar, Hatch 2001)

Recycled and fresh cumene is the inlet flow for the first reactor. Air is fed in and bubbled from the reactor bottom and it leaves the reactor from the top. Pressure conditions for the oxidation reactors are low or moderate. External cooling removes the heat that is generated by the oxidation reaction (Chianese 1982).

Through the reaction of a portion of cumene dimethylbenzyl alcohol and acetophenone are formed. Methanol that is formed in the acetophenone reaction is turned into formaldehyde and formic acid by oxidation. Water is also formed by reactions, but its amount is small. The selectivity of the reaction depends on residence time, temperature, oxygen partial pressure and conversion level. The yield of the CHP is 95 % mol during the oxidation step. Cumene that did not react is stripped out and returned into the production as a recycle flow that goes into the first oxidation reactor. 99.99 % of cumene and some organic compounds are recovered by treatment of the exhaust air (Matsui, Fujita 2001).

The cleavage reactor is fed by the concentrated CHP after cumene stripping. The cleavage reaction of CHP to acetone and phenol with acid catalyst runs by ionic mechanism. This reaction can be found in Figure 3. Sulfuric acid is used as catalyst for the cleavage reaction.

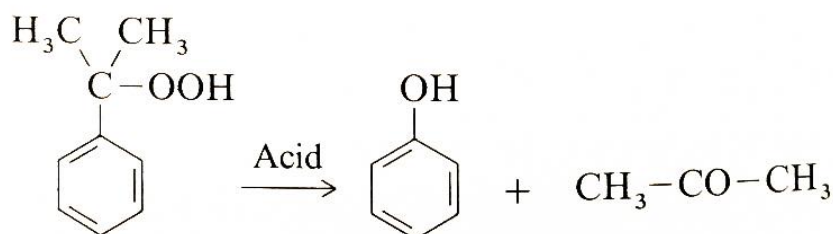


Figure 3 Obtaining phenol by CHP cleavage with acidic medium (Matar, Hatch 2001)

The cleavage with acid catalyst runs in two ways. The excess of acetone is put into the cleavage reactor in homogeneous phase. 0.1-2 % of sulfuric acid is required for the cleavage reaction. The reaction temperature is equal to the boiling point of CHP-acetone mixture. The boiling temperature depends on the composition of the mixture. Optimum temperature is maintained by changing the cleavage reactor conditions to maximize phenol yield (Chudinova, Salischeva et al. 2015).

In the heterogeneous phase reaction, CHP is cleaved by 40-45 % sulfuric acid at an acid-concentrate ratio of 5:1. The compounds are mixed in a centrifugal pump. The generation of by-products is limited by short residence time of about 45-60 s. Special chromium steel with alloyed copper is used to avoid corrosion (Levin, Gonzales et al. 2006).

The process of the CHP cleavage runs until the residual concentration of less than 0.1 % is gained. Most a-dimethyl benzyl alcohol formed during the oxidation process is dehydrated to AMS. 4-cumylphenol and mesityl oxide are typical by-products of the acidic cleavage reaction (Di Somma, Andreozzi et al. 2008).

Commercial yield of phenol in cumene process is typically more than 98 % mol. The acid is used as catalyst with acetic and formic acids being by-products of the reactions. That is why these acids must be neutralized and removed in order to avoid corrosion. The neutralization process can be carried out by using aqueous phenolate solution or aqueous sodium hydroxide. Water that contains the salt is removed from the reaction mixture (Wallace, Updated by Staff 2000).

In distillation columns products received after cleavage reaction are separated. The mixture contains phenol, acetone, organic impurities, hydrocarbons and water. AMS at this section can be hydrogenated to cumene or separated as a product. Many plants of phenol production include special water treatment units to remove phenol and acetone from wastewater due to the negative impact these products may bring to the environment (Busca, Berardinelli et al. 2008).

In short, the cumene process may be described in the following way: a typical phenol production plant based on the cumene process includes two principal parts. The reaction part includes oxidation of cumene formed by alkylation process of propylene and benzene in order to form CHP. After that, acetone and phenol are produced by using the CHP. Dimethylbenzyl alcohol and acetophenone are by-products that are formed during the oxidation reaction. AMS is formed by dehydration of dimethylbenzyl. The second part includes purification to commercial acetone and phenol. This recovery part also includes the recovery flow of AMS that can be transformed back to cumene by hydrogenation or can be recovered as a product as such (Zakoshansky 2007). Figure 4 demonstrates another simplified block diagram of the process.

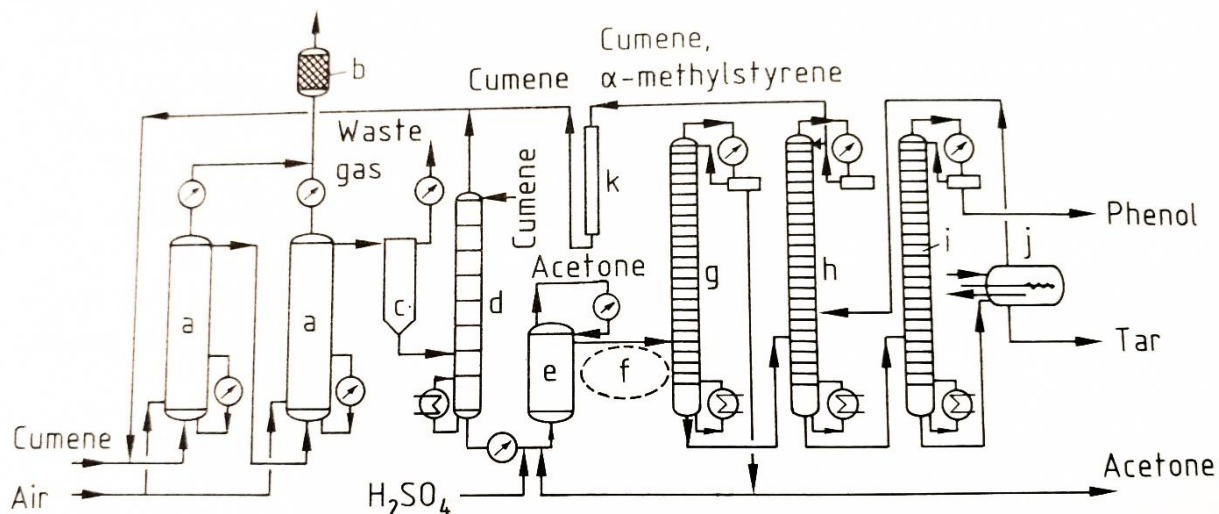


Figure 4 Typical phenol production from cumene. a) Oxidation reactor for cumene; b) Waste gas purification; c) Gas separator; d) Concentration; e) Reactor for cleavage reaction; f) Catalyst separation; g) Column for acetone separation; g) Column for cumene separation; i) Column for phenol separation; j) Cracking; k) Hydrogenation (McKetta Jr 1990)

### 2.3 Toluene and benzoic acid process

Dow-Canada, Ltd. were first to introduce the toluene and benzoic acid process in 1961, which accounts for about 4 % of the world's synthetic phenol production capacity (Schmidt 2005).

There are three main reactions in toluene and benzoic acid process. The first one is toluene oxidation to benzoic acid, the second is benzoic acid oxidation to phenyl benzoate, and the third is phenyl benzoate hydrolysis to phenol (Liu, Lu et al. 1998). A typical toluene and benzoic acid process includes two continuous steps. The first step is the toluene oxidation to form benzoic acid. The reaction runs with cobalt salt and air as catalysts at the temperatures between 121 and 177 °C. The concentration of the catalyst varies between 0.1 and 0.3 % mass. The reaction takes place under the pressure of 307 kPa in the reactor. After that benzoic acid is distilled from the flow. The yield of the toluene and benzoic acid process is about 68 % mol (Wallace, Updated by Staff 2000). Steps of the toluene and benzoic acid process can be found in Figure 5.

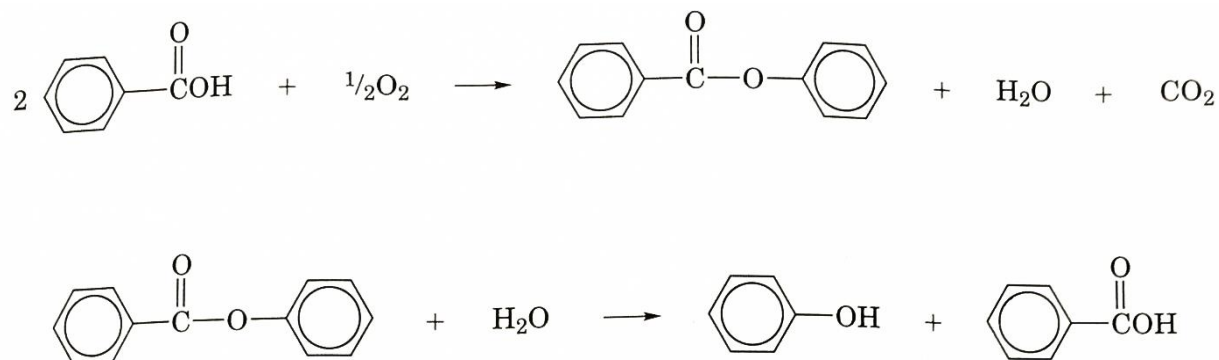


Figure 5 Toluene and benzoic acid production of phenol (McKetta Jr 1990)

The second step of the process includes oxidation and hydrolyzation of benzoic acid to phenol and takes place into two reactors. In the first reactor oxidation of benzoic acid to phenyl benzoate runs with a catalyst mixture of magnesium and copper salts and air. The reaction is done under the temperature of 234 °C and the pressure of 247 kPa in the reactor. After that the mixture goes into the second reactor, where phenyl benzoate is hydrolyzed by steam to carbon dioxide and phenol. The reaction runs under the temperature of 200 °C and atmospheric pressure. The phenol yield from benzoic acid is about 88 % mol (Grbić-Galić, Vogel 1987). Figure 6 shows a block diagram of the toluene and benzoic acid process.

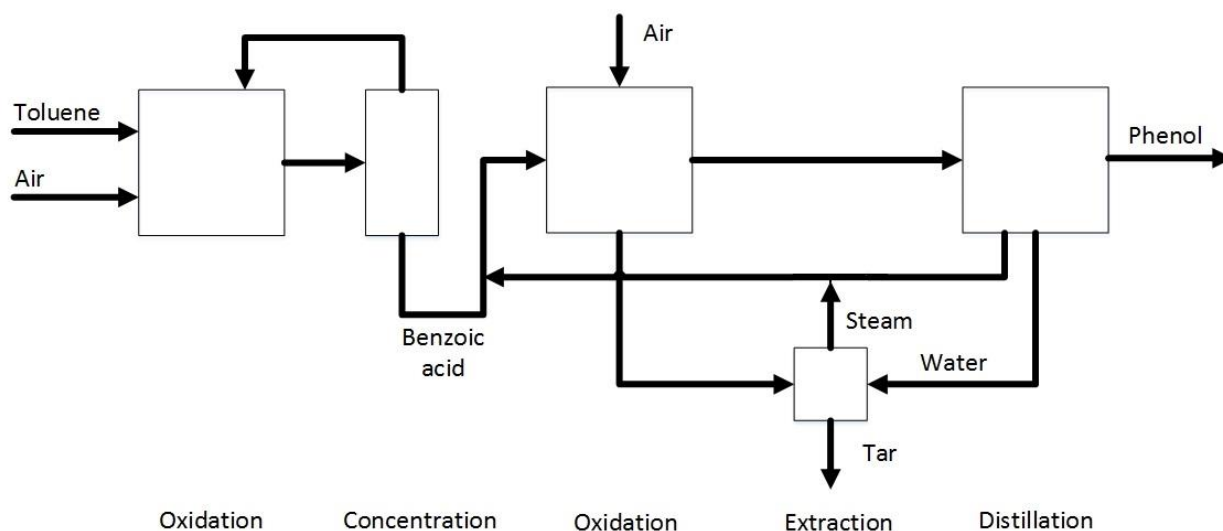


Figure 6 Block diagram of toluene and benzoic acid production of phenol (McKetta Jr 1990)

## 2.4 Modern alternatives of phenol production

The usage of alternative technologies of phenol production instead of the cumene process may become an option for solving the issue of phenolic resin disposal. This part considers a few

alternative technologies of phenol production to find out whether they may serve as possible solutions to the issue, otherwise the efficiency of the cumene process will be justified.

There are a few alternative ways of phenol production. Some of them are outdated and have low economic efficiency, that is why they are almost never used. For instance, there is a technology of phenol production through cyclohexane or from benzene by sulphonation and direct chlorination. Such outdated technologies are still used at some plants mainly to satisfy local needs. For example, the toluene method is used in three small-scale plants in the Netherlands and Japan (Schmidt 2005).

The joint production of acetone and phenol poses one common problem. The fact is that by most methods more acetone than phenol is produced. In the industry, significant amounts of phenol and acetone are used to produce carbonate plastics, where only one mole of acetone is required for two moles of phenol. Other industries, however, are not able to use the rest of acetone. Therefore, the industry seeks decisions discouraging strong imbalance between phenol and acetone (Pillai, Jia et al. 2004). Another objective of such promising alternative methods of phenol production is to reduce capital costs and costs of production, as well as to reduce or eliminate ecological impact caused by production. The list of preferable methods of phenol production is the following (Balducci, Bianchi et al. 2003, Zakoshansky 2009, Ren, Yan et al. 2003, Nexant Chem Systems 2006, Yang, Black et al. 2006):

- a) direct benzene oxidation to phenol
- b) benzene oxidation with  $N_2O$  to phenol
- c) joint production of phenol and methylethylketone
- d) increasing the selectivity of the cumene process in order to increase the yield of phenol
- e) involvement of acetone in other areas of synthesis, including conversion of acetone to propylene

Alternative methods of phenol production without acetone may also be quite perspective but they pose two major problems. The first problem is that the demand for acetone still remains to produce a range of plastics and other products. The second problem is that there are many plants that use cumene method of phenol and acetone production with a total capacity of more than 12.5 million tons per year (ICIS 2016), which means that phasing such plants out to replace them by ones using alternative methods is not economically feasible. However, it is highly important to study alternative technologies in order to understand future perspectives and be able to compare the level of achievable selectivity with the selectivity of the cumene process.

### **2.4.1 Direct oxidation of benzene to phenol**

This method of direct benzene oxidation to phenol is of interest because it is only a one-stage process. In this regard, two directions of direct benzene oxidation should be distinguished. These are hydroxylation with hydrogen peroxide and oxidation by air oxygen (Burch, Howitt 1992).

Oxidation with hydrogen peroxide has a few disadvantages. First, hydrogen peroxide as such is quite costly, which makes the whole process expensive. Second, hydrogen peroxide is a harsh oxidizing agent, which determines the low selectivity of the reaction for benzene, and even more so for  $\text{H}_2\text{O}_2$ . The produced phenol is oxidized with hydrogen peroxide, and such by-products as hydroquinone, resorcinol, pyrocatechin are derived in the result. It is almost impossible to avoid by-products, as the reactivity of phenol and its derivatives is much higher than the reactivity of benzene (Yang, Sun et al. 2013). Thirdly, the process brings certain amount of negative environmental impact since a lot of wastewater contaminated with traces of phenol is left after the process is done (Ohkubo, Kobayashi et al. 2011). What is more, hydrogen peroxide production is quite laborious and energy consuming. Apart from the negative points mentioned above, it should be mentioned that during the phenol process most hydrogen peroxide turns into water. And finally, large-scale production of phenol demands large amounts of hydrogen peroxide, which requires construction of more industries producing hydrogen peroxide (Balducci, Bianchi et al. 2003).

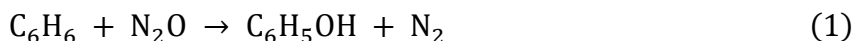
The direct oxidation of benzene with air oxygen has also a number of disadvantages. First, it can be achieved only by low conversion of the feedstock (benzene) due to the difference in reactivity of the feedstock (benzene) and the final product obtained (Liu, Murata et al. 2006). Other deficiencies include a large amount of recycle streams, difficulties with separating the reaction products and ensuring the stability of the catalyst, as well as significant amounts of production waste. These disadvantages of the presented methods do not allow making this method competitive with respect to the cumene process (Taboada 2006).

### **2.4.2 Oxidation of benzene by $\text{N}_2\text{O}$ to phenol**

There are two processes of benzene oxidation to phenol by using  $\text{N}_2\text{O}$ . The first method is called VTOR. It is aimed to solve a local problem, namely disposal of hazardous waste ( $\text{N}_2\text{O}$ ) that is produced during the adipine formation. The second process is called AlphOx, and it is used to solve more vast problems such as entering the global market of phenol. The process opponents claim that it is a simpler, cheaper and more environmentally friendly way than the traditional cumene process of phenol production. During the process  $\text{N}_2\text{O}$  is obtained from  $\text{NH}_3$

(Kachurovskaya, Zhidomirov et al. 2004). It should also be mentioned that the VTOR process is an integral part of the AlphOx process.

The main reaction of the VTOR process is given by Eq. 1:



Potential advantages of the VTOR process compared with the cumene process (Ren, Yan et al. 2003):

- a) the waste ( $\text{N}_2\text{O}$ ) of adipine production has its application, which reduces the cost of phenol production under the VTOR process, and at the same time influences positively on the ecology of adipic acid production;
- b) propylene is not required;
- c) no alkylation of benzene with propylene is required, which simplifies the process greatly;
- d) acetone is not produced in the process;
- e) the dangerous product of CHP is completely rejected.

In terms of its implementation, the VTOR process advanced further than the direct oxidation of benzene. It passed pilot tests, and AlphOx technology was tested on a pilot plant of Solutia in Pensacola, Florida.

After closer view at the technology, however, it turns out that this process is not as simple as it may seem first. The VTOR process, like the cumene process, is multistaged in its chemistry and technology. It includes (Zakoshansky 2009):

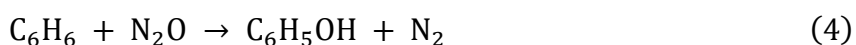
- a) a complex stage of purification of  $\text{N}_2\text{O}$  received from NO and other nitrogen-containing gases;
- b) the high-temperature stage of benzene oxidation with the chemically “hard” oxidizing agent  $\text{N}_2\text{O}$ ;
- c) the chemical stage of catalyst regeneration;
- d) the catalytic stage of conversion and purification of a gas mixture containing unreacted  $\text{N}_2\text{O}$ , oxygen, nitrogen, CO and the product of incomplete reduction of  $\text{N}_2\text{O}$ , namely nitrogen oxide NO;
- e) the chemical stage of phenol purification.

One of the disadvantages of this method is that a few by-products are produced in the process. The fact is that using a strong oxidizing agent ( $\text{N}_2\text{O}$ ) at a high temperature of 400-450 °C leads to inevitable production of impurities. The method also poses the issue of the colority, because it is

difficult to provide the necessary colority at high temperatures with a strong oxidizing agent (Hensen, Zhu et al. 2005). Samples from the pilot plant did not pass the test for colority, which challenges the possibility of using this phenol for carbonate plastics and for wood processing. Thus, the stage of phenol purification in this process is more complicated than in the cumene process, despite the fact that a larger number of distillation columns is used in the last one. It should be mentioned that the pilot tests were carried out for a small scale of phenol (0.4 kg/h phenol), though it is important to understand that phenol production of should be large-tonnage. Therefore, one cannot claim that there will be no problems with transferring of this technology to large-tonnage production (Gopalakrishnan, Münch et al. 2006). Another problem is the high rate of deactivation of the catalyst due to its coking. In this process, the catalyst must be regenerated every 3-5 hours (Ren, Yan et al. 2003), that is why it is necessary to build many reactors (Pillai, Jia et al. 2004). Moreover, there is a possibility of only partial conversion of N<sub>2</sub>O, resulting in the catalyst activity decrease during the contacting cycle, as well as in the selectivity for benzene and for N<sub>2</sub>O decrease. The selectivity of the process is 90-99 % (Fellah, van Santen et al. 2009). The practice of many industrial processes has shown that many processes operate at a lower selectivity than the one that was in the project. The selectivity for the second reagent is 70-80 % and depends on the temperature. Such value of selectivity is quite low, as well as the selectivity of the oxidation of ammonia in N<sub>2</sub>O (Hiemer, Klemm et al. 2004).

It is possible to use practically free N<sub>2</sub>O in adipic acid production, however the production capacities of the industries are not enough to resolve the imbalance in phenol and acetone production. According to the data on adipic acid production, adding phenol production with the VTOR technology to the plants will allow to reduce the imbalance of acetone and phenol by 5 %. It is worth mentioning that not all of the adipic acid productions will agree to add phenol production. That fact reduces from 5 to 1-2 %. The construction of production with the VTOR process is economically feasible only for large adipic acid productions (Uriarte 2000). Construction of the phenol production for medium- and small-scale adipic acid producers is not economically efficient. Due to the disadvantages of the VTOR process, the AlphOx process was introduced. This process involves the production of N<sub>2</sub>O from NH<sub>3</sub> (Notté 2004).

AlphOx process chemical reactions without adverse reactions are given by Eq. 2-4:



The selectivity of the first reaction is 93 % mol. The selectivity of the second reaction is 80 % by  $\text{NH}_3$  and 88 % by  $\text{O}_2$ . The third reaction has the selectivity of 95% by benzene and 70-80 % by  $\text{N}_2\text{O}$ .  $\text{N}_2$  is nitrogen contaminated with nitrogen oxides, carbon oxides, etc (Zakoshansky 2009).

In this process, the nitrogen hydrogen and oxygen are taken as the consumed raw material. Nitrogen is taken from the air. Hydrogen is obtained by processing raw organic materials or by water electrolysis. Oxygen is also taken from the air. All of the above is used to get  $\text{N}_2\text{O}$ . The received NO reacts with benzene. As a result of this reaction a few products are produced, with phenol being the main product and such by-products as nitrogen and water (Li, Feng et al. 2008).

The technological features of the AlphOx process include several stages. All hydrogen used in the process is converted to water. The pure nitrogen produced from the air is converted into environmentally polluted nitrogen, which is thoroughly cleaned mainly from NO and CO. The mass ratio of the products and by-products is 0.9:1. The total nitrogen selectivity used as a feedstock is about 50 %, which is quite a low percentage (Parmon, Panov et al. 2005).

A significant disadvantage of the AlphOx process is that compared to the VTOR process, there is the larger number of stages, leading to the increase in the capital and operational costs. It is also worth mentioning that the feedstock in the form of hydrogen and nitrogen is converted into waste products of water and dirty nitrogen, the purification of which also requires energy and equipment. What is more, the problem poses the fact that the volume of waste products produced is comparable to the production of phenol (Hensen, Zhu et al. 2004). Probably, the implementation of this production in arid areas would be a good solution, since a lot of water is produced in this production. However, this decision does not solve the problem of polluted nitrogen. The approximate product yields are 230 t of water and 114 t of polluted nitrogen per 400 t of produced phenol (Meloni, Monaci et al. 2003). This process leaves significant environmental footprint, since a lot of wastewater is produced over the course. About 0.6 t of wastewater per a ton of phenol is produced. Nitric oxide is partially soluble in water, and nitrogen dioxide reacts with water. This reaction is given by Eq. 5 (Zakoshansky 2009):



This fact justifies the large amount of wastewater, inevitably bringing harm to the environment. Compared to the cumene process, the AlphOx process is technologically more complex and expensive, since operational and capital costs increase significantly due to the shortcomings of the method. The main disadvantage of the process is the number of steps. Moreover, only 50 % of the necessary products are produced, with water and crude nitrogen being the rest 50 % of production. For this reason, additional money is needed to be allocated for purification, which significantly

increases the cost of overall production (Pirutko, Uriarte et al. 2001). What is more, the water produced is not an expensive product, which makes its production completely unprofitable, while acetone costs high in the production of the cumene process. It is also worth mentioning that solving the problem of acetone oversupply is possible only with building new capacities for ammonia production, since there is no excess ammonia on the market. Considering that the required amount of H<sub>2</sub> on the market is not also available, additional construction of production is required. Thus, capital costs and operational costs increase significantly (Leanza, Rossetti et al. 2001).

### 2.4.3 Joint production of phenol and methylethylketone

This method is similar to the cumene method, but methylethylketone is obtained in the process instead of acetone. The simplified scheme without adverse reactions can be found in Figure 7.

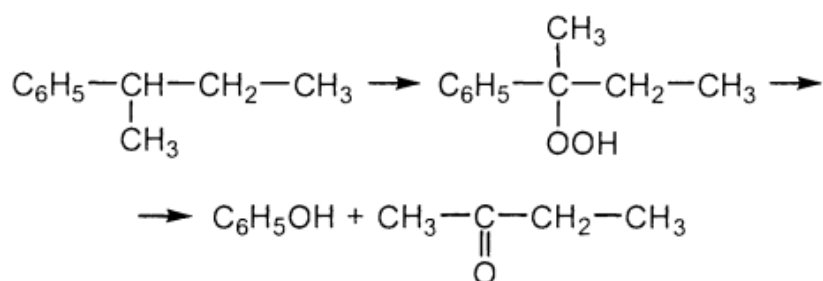


Figure 7 Reactions of joint production of phenol and methylethylketone (Zakoshansky 2009)

At first glance, this process may perfectly replace part of phenol and acetone production and thus solve the problem of excess acetone. Moreover, the methylethylketone produced by this method is approximately twice as expensive as acetone. The cost of propylene is about two times higher than the cost of butylenes needed to produce sec-butylbenzene, since butylenes cannot be used individually, however their mixture consisting of butene-1, butene-2 and isobutylene can. It should be mentioned that not all refineries are concerned with finding the ways to profitably dispose the mixed butenes, that is why profitable production of expensive sec-butylbenzene will be a relevant method of disposal for them. It cannot be claimed that today's market is oversaturated with methylethylketone, however the large production of phenol will ensure the production of methylethylketone exceeding the demand for this substance (Palma, Paiva et al. 2007). The conversion of existing phenol and acetone production by the cumene method to the process of phenol and methylethylketone production is impossible, since the processes, despite they seem quite similar, differ in the rates of chemical reactions and in the number of by-products produced. Apart from that, the by-products formed in phenol and methylethylketone production have their problems in the separation and purification stages (Cheng, Buchanan et al. 2010).

The stage of oxidation of sec-butylbenzene with atmospheric oxygen compared with the similar stage of cumene oxidation is performed at purposely high temperatures of 125-130 °C. It is necessary to achieve the oxidation rate of sec-butylbenzene acceptable for the process, which is approximately two times lower than the rate of cumene oxidation (Nexant Chem Systems 2006). However, the solution of this problem by increasing the temperature leads to the next problem of many by-products produced, including strong organic acids. This, in its turn, initiates the formation of an inhibitor, phenol, which slows down the process and does not allow increasing of sec-butylbenzene conversion. These problems happen due to the peculiarity of sec-butylbenzene structure, its activation parameters and side reactions. The approach of neutralizing the formed organic acids with NaOH, which is used in traditional technologies for the oxidation of cumene, does not help to increase sec-butylbenzene oxidation rate or to increase its conversion to the enough value for usage in industry (Yang, Black et al. 2006).

It was proposed to combine the cumene process with the production of phenol together with methylethylketone. However, the number of trace impurities including undesirable carbonyl compounds formed in this combined process, adversely effect on the quality of the phenol produced. The quality of phenol produced in such a way is several times lower than the quality of the phenol formed by the cumene process, which leads to increasing energy consumption and capital costs compared to the cumene process. Moreover, the process of products purification from impurities is complicated. The separation stage is more complicated than at the cumene process not only because of new impurities. In the process of methylethylketone and phenol production three products are derived, namely phenol, acetone and methylethylketone, while only two of them are obtained in the cumene process. There are more problems at purification of methylethylketone stage than at purification of acetone stage, since acetone mixes with water and forms an azeotropic mixture. The combined process has negative environmental impact due to the huge number of aldehydes and organic acids derived at the oxidation stage and the huge amount of non-utilizable waste produced at the decomposition stage (even in the case of cracking and incineration of residues) (Fathi-Afshar, Rudd 1981). Methylethylketone has a strong odor, which leads to the problems when even a small amount of a substance enters the atmosphere. These factors make the combined process of obtaining phenol and methylethylketone more complicated than the cumene process in terms of capital and operational costs, as well as in terms of ecology. These shortcomings will not allow wide distribution of this technology, which in its turn will not solve the imbalance in acetone and phenol production. However, the uncombined process with the cumene process may still be an option, but there is not enough data to accurately analyze the prospects of this method so far (Dakka, Levin et al. 2008).

#### **2.4.4 Conclusion on modern alternative processes**

Alternative acetone-free technologies of phenol production have not been brought to a level that would allow them to be commercialized. The modern cumene process of phenol and acetone production has reached the maximum possible level of selectivity, namely 97 % mol. All the issues concerning the quality of the final products have been resolved. (Zakoshansky 2009). The level of safety and environmental protection meets modern requirements. The cumene process remains the predominant technology for the coming decades.

### 3 Phenolic resin processing

Conversion of waste stream into products is a method to increase the process efficiency. Phenolic resin is the main waste of phenol and acetone production, and the main objective of its processing is to turn phenolic resin into phenol, cumene and AMS. The amount of phenolic resin depends on particular technology of cumene method, beginning from 150 to 250 kg per ton of the phenol. The lack of phenolic resin processing means the loss of more than millions of tons of raw material. The second significant problem concerns the ecological impact caused by phenolic resin disposal (Gardziella, Pilato et al. 2013).

#### 3.1 Phenolic resin processing methods

Vast research has been done concerning disposal of phenolic resin and its components. There are two main strategies. The first strategy concerns the usage of phenolic resin without pretreatment, and the second is aimed at phenolic resin processing at phenol production. The first group includes the following ways of phenolic resin disposal (Zárate, Aranguren et al. 2008, Pilato 2010, Correia, de Carvalho 2003, Zakoshansky 2007, Schmidt 2005, Knop, Pilato 2013):

- a) to use phenolic resin as flotation reagent or additive for these reagents;
- b) to inject phenolic resin into subsurface in order to increase oil recovery;
- c) to use phenolic resin as additive for lubricating oils;
- d) to use phenolic resin as additive for concrete in order to achieve plasticity and increase its quality;
- e) to use phenolic resin for healthcare products for large cattle breeding;
- f) to use phenolic resin as additive for diesel fuel in order to decrease its price;
- g) to use phenolic resin for technical carbon production that is needed for high quality electrodes.

Unfortunately, all these methods are not spread widely, but some of them are used to satisfy local needs. The main problem is posed by the fact that the ecological issue is not solved at phenol and acetone production plants. That means that these methods provide profitable ways of phenol resin disposal from phenol and acetone production, while ignoring the problem from the point of ecology (Loos 2000). The second group of phenolic resin disposal methods includes the following methods (Zakoshansky 2007):

- a) increasing the amount of commercial phenol by additional distillation of phenolic resin;
- b) using thermal cracking to turn phenolic resin into products;
- c) using heterogeneous acid catalysts for catalytic cracking of phenolic resin;

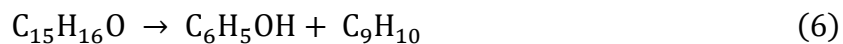
- d) burning phenolic resin in order to get steam;
- e) a combination of thermal cracking and burning of phenolic resin.

Catalytic cracking is the only technology that is not used in existing phenol and acetone productions, because the industrial tests of this technology have failed, despite satisfactory laboratory experiment results (Meikrantz, Bourne et al. 1991). Phosphoric acid, polyphosphoric acids, aluminum and sodium phenolate and other acids and bases may be used as possible catalysts for catalytic cracking of phenolic resin. Adding of small amount of water may improve cracking and increase yield of the products (Levchik, Weil 2004). During the usage of heterogeneous catalysts, products of deep condensation clad acid particles of catalyst, which leads to low conversion of AMS dimers and cumylphenols. As a result, the amount of received phenol, AMS and cumene is low, that is why it can be claimed that the attempts to work with heterogeneous catalysts did not prove to be successful. The usage of different homogeneous acid catalysts or alkaline catalysts is problematic, since it leads to spoiling of products because of catalysts. Apart from that, with the presence of catalysts recycle phenolic flows may spoil full production chain (Pilato 2010).

All the methods of phenolic resin disposal require pretreatment, mostly to remove salts. Salts contained in phenolic resin make disposal more complicated, as they may spoil the equipment. Since the problem of phenolic resin purification from salts has been solved, there is an opportunity to use thermal cracking and burning for phenolic resin processing bringing no harm to the equipment.

### 3.2 Thermal cracking of phenolic resin

The reactions for main components of phenolic resin run in thermal cracking of phenolic resin (cumylphenols and AMS dimers) are given by Eq. 6-9 (Zakoshansky 2007):



Though hydrogen is not added to the reactor, though it is present in the process since it is produced in the thermal cracking process. Acetophenone is also formed at high temperatures during thermal cracking from dimethylphenylcarbinol and as a result of cumylphenols decomposition. Acetophenone, that is present in phenolic resin and is formed during the process, takes part in the reaction with phenol and in condensation reaction in which resin products lead to the loss in phenol. Most organic acids enter the reactor with phenolic resin. Organic sulphur-containing

products appear in the composition because of thermal decomposition reactions with  $\text{Na}_2\text{SO}_4$  in which  $\text{SO}_2$  and  $\text{SO}_3$  are formed and later interact with phenolic resin components under high temperature into the reactor (Zárate, Aranguren et al. 2008). Strong organic acids, mostly formic acid and mineral acids make productions to use stainless steels or highly alloyed steels for equipment. This fact leads to the increase in capital costs. The yield of useful products, such as phenol, AMS and cumene, is 40-50 % mass from the potential amount of phenolic resin that goes into the reactor of thermal cracking (Tzeng, Chr 2002). The reactor is heated by natural gas. Despite the high temperature of the process, which is not less than 300 °C, and high residence, namely between 10 and 30 h, the yield of the process is low (Zakoshansky 2007). Changing the residence time and temperatures has not proved to give satisfactory results, because reducing of these parameters decreases conversion of the cracking products. The temperatures higher than 300 °C lead to coking, which influences negatively on the process (Correia, de Carvalho 2003). Catalytic cracking can be used to increase the yield of the products from phenolic resin, but this process has its negative sides (Wang, Adanur et al. 1997). Catalytic cracking is a complicated process and it influences negatively on phenol and acetone production because of the catalysts and other issues. That is why it is not profitable to increase the yield by 10 % (Knop, Pilato 2013).

There are also minor reactions by which cumene, benzene, toluene, ethylbenzene and other alkylbenzenes are formed during the thermal cracking process. What is more, thermal conversion of cumylphenols leads to cresols and methanol formation, while conversion of products of aldehyde deep condensation leads to aldehyde formation. All these minor products of thermal cracking are returned into the process of phenol and acetone production, which leads to decrease in commercial phenol and acetone quality (Bender, Farnham et al. 1952). As a result, extra capital costs are needed to distillate products and reduce negative quality effect after thermal cracking. Despite the advantage of increasing the number of products there are several disadvantages of using thermal cracking. First, it is the increase in steam consumption which leads to higher operational costs. Second, it is the fact that commercial phenol and acetone quality is reduced, making distillation more expensive. Third, there is a need in more equipment for phenolic resin processing, which also contributes to the increase in capital costs. Finally, the main issue of thermal cracking is its complex operational aspect, because the process of cracking is complicated and requires regular equipment maintenance (Bahramian, Kokabi et al. 2006). All the mentioned disadvantages confirm the idea that thermal cracking is not the most profitable option for phenolic resin disposal, though it has proved to be the best among the methods known so far.

## EXPERIMENTAL PART

### 4 Phenolic processing unit process design

This chapter describes the development of phenolic resin processing unit that would turn waste stream into products. This gives an opportunity to reduce production waste and to obtain new products that may increase production profits.

The best way to get products from phenolic resin is catalytic cracking according to methods of phenolic resin processing and disposal that were described above. But the disadvantages of the method do not give an opportunity to use it in phenol and acetone production. The main issue is that there are many by-products with heterogeneous catalysts, which leads to low conversion of products. It is impossible to use homogeneous catalyst because the products are spoiled by the presence of catalysts. What is more, the phenolic fraction flow that will be returned to production with the presence of catalysts will spoil the full production chain. That is why it was decided to use thermal cracking process instead. A reactor with three distillation columns was chosen as the layout of the phenol resin processing unit. Figure 8 shows where the place of phenolic resin processing unit in the phenol and acetone production.

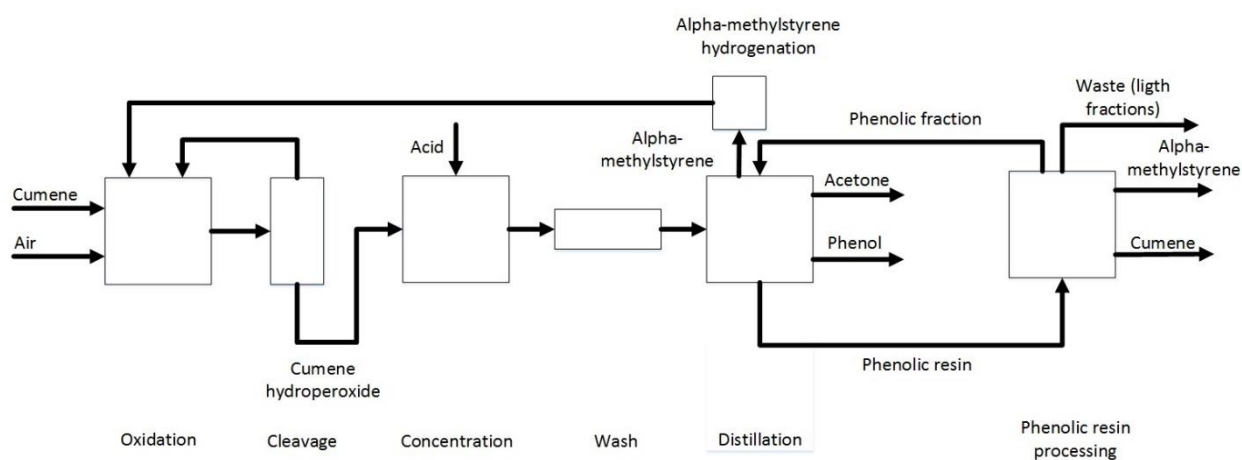


Figure 8 Phenol production by cumene process with phenolic processing unit

## 5 Simulations

### 5.1 Simulation of phenol-acetone distillation with Aspen Hysys

It was decided to start simulations from the step of phenol and acetone production before proceeding to phenolic resin processing. Typical phenol and acetone separation scheme with average capacity for phenol production was taken as initial data (Romanova, Leontiev 2017). Typical capacity for phenol production by cumene process is 200000 t/year of phenol and 125000 t/year of acetone (INEOS Phenol 2019, ICIS 2016, Borealis 2019). This simulation is required for validating the method of phenolic resin processing unit simulation. It also provides the opportunity to assess the increase in phenol as it will be purified to commercial quality in the distillation step of phenol and acetone production. Moreover, this simulation will give information about heat flows, which are needed for pinch analysis necessary for heat integration system design.

### 5.2 Phenol-acetone distillation process description

The diagram of the distillation step of acetone and phenol can be found in Figure 9.

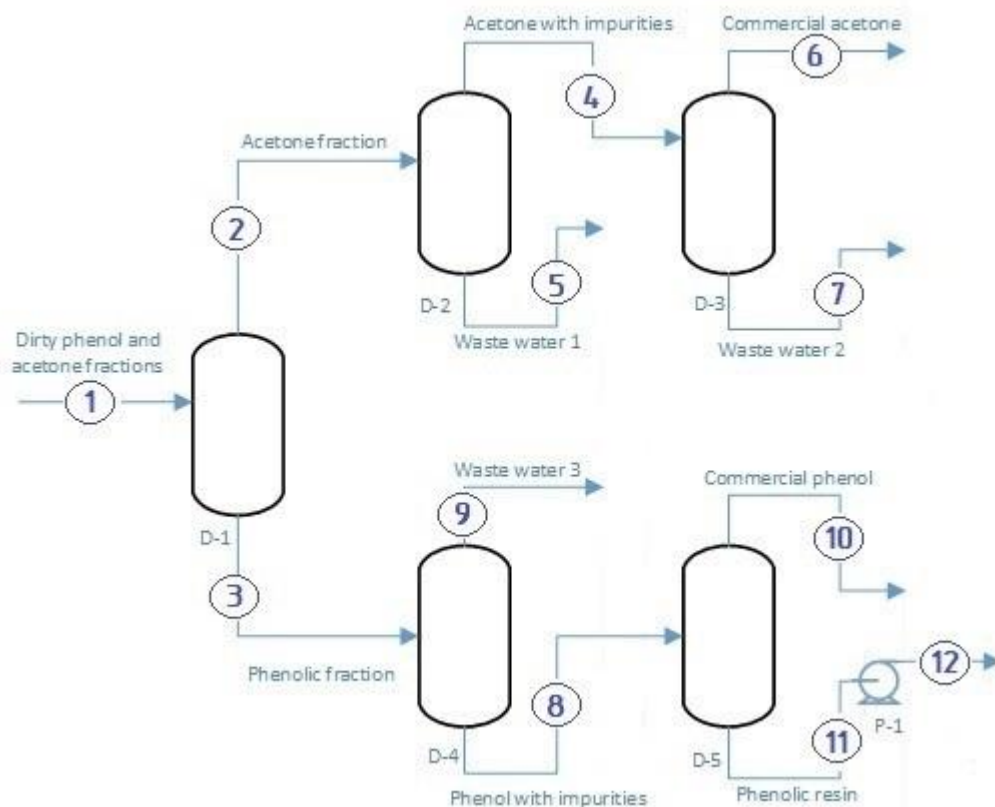


Figure 9 Typical diagram of phenol and acetone distillation at phenol production by cumene method (Romanova, Leontiev 2017)

The first column D-1 separates the phenol fraction with heavy impurities from the acetone fraction. The distillate of column D-1 goes into two-step distillation in columns D-2 and D-3. The distillate of column D-3 is commercial acetone, and its waste stream is waste water (Kujawski, Warszawski et al. 2004). Columns D-4 and D-5 help to remove impurities from the phenol fraction. Finally, the distillate of column D-5 is commercial phenol, and its waste stream is phenolic resin. Simulation of the distillation scheme in Aspen Hysys is presented in Figure 10.

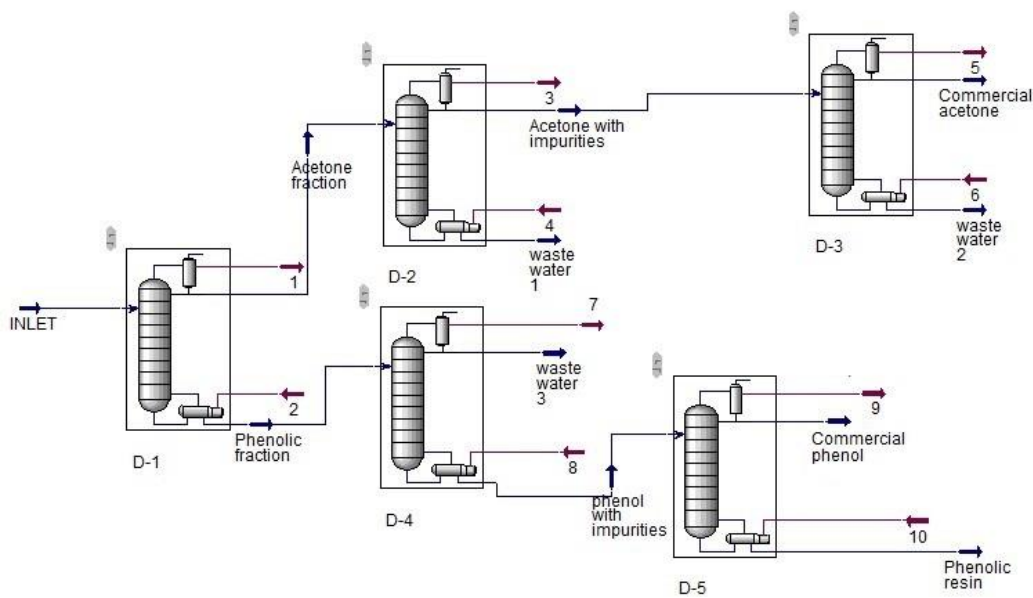


Figure 10 Simulation of phenol and acetone distillation in Aspen Hysys

First step of the simulation is selection of the thermodynamic package. NRTL was selected as the estimation model because it serves to simulate the non-ideal behavior in the liquid phase and it is used for aqueous organics (Suppes 2002). NRTL is used for simulations that are related to cumene process, such as acetone and phenol separation (Andrigo, Caimi et al. 1992, Romanova, Leontiev 20115, Mafra, Krähenbühl 2006, Cepeda, Gonzalez et al. 1989). Heat flows for pinch analysis were obtained after the simulation. Column parameters are present in Table VII. Mass balances can be found in Table VIII.

Table VII Distillation column parameters for phenol and acetone separation

Column	D-1	D-2	D-3	D-4	D-5
Number of stages	16	35	58	18	22
Feed stage (top-down numbering)	8-12	23-29	49-55	10-16	8-13
Reflux ratio	0.6	2.1	5.0	1.1	5
Distillate rate	0.46	0.64	0.98	0.08	0.82
Pressure, kPa	120	50	40	20	10

Table VIII Mass balance for phenol and acetone separation

	1	2	3	4	5	6
Description	Acetone and phenol fraction	Acetone fraction	Phenolic fraction	Acetone with impurities	Waste water 1	Commercial acetone
Acetophenone, kg/h	736.3	48.0	688.3	0.0	48.0	0.0
Phenol, kg/h	22836.8	1.2	22835.7	0.0	1.2	0.0
Para-Cumylphenol, kg/h	578.0	0.0	578.0	0.0	0.0	0.0
AMS, kg/h	1983.8	1755.8	228.0	0.0	1755.8	0.0
Cumene, kg/h	833.6	825.7	7.9	0.0	825.7	0.0
Water, kg/h	7020.0	5225.4	1794.6	68.2	5157.2	4.4
Acetone, kg/h	14249.0	14243.9	5.2	14131.8	112.1	13995.5
Total, kg/h	48237.5	22099.9	26137.7	14200.0	7899.9	14000.0
Pressure, kPa	150.0	120.0	160.0	50.0	65.0	40.0
Temperature, °C	60.0	66.0	133.0	37.0	79.5	31.0

Table VIII (continued) Mass balance for phenol and acetone separation

	7	8	9	10	11	12
Description	Waste water 2	Phenol with impurities	Waste water 3	Commercial phenol	Phenolic resin	(Pumped) Phenolic resin
Acetophenone, kg/h	0.0	1279.2	0.0	0.0	1279.2	1279.2
Phenol, kg/h	0.0	23339.0	3.2	21180.5	2158.5	2158.5
Para-Cumylphenol, kg/h	0.0	1192.4	0.0	0.0	1192.4	1192.4
AMS, kg/h	0.0	14.2	324.7	14.2	0.0	0.0
Cumene, kg/h	0.0	0.0	8.3	0.0	0.0	0.0
Water, kg/h	63.7	0.0	1794.6	0.0	0.0	0.0
Acetone, kg/h	136.2	0.0	5.2	0.0	0.0	0.0
Total, kg/h	200.0	25824.9	2136.0	21194.7	4630.1	4630.1
Pressure, kPa	60.0	32.0	21.0	10.0	22.0	172.0
Temperature, °C	44.0	145.5	48.0	113.5	147.0	147.0

Energy balances can be found in Table IX. The numbering of heat flows was given in Figure 10.

Table IX Energy balance for phenol and acetone separation

Column	Energy flow	Heat flow, kJ/h	Power, kW
D-1	1	$3.20 \cdot 10^7$	8887.0
	2	$3.65 \cdot 10^7$	10150.3
D-2	3	$2.31 \cdot 10^7$	6428.4
	4	$2.26 \cdot 10^7$	6270.7
D-3	5	$4.39 \cdot 10^7$	12190.2
	6	$4.37 \cdot 10^7$	12150.3
D-4	7	$9.04 \cdot 10^6$	2512.0
	8	$8.45 \cdot 10^6$	2347.0
D-5	9	$6.77 \cdot 10^7$	18810.4
	10	$6.63 \cdot 10^7$	18400.3

### 5.3 Reactor simulation: Aspen Plus

The first step in the phenolic resin processing unit is the thermal cracking reactor that increases the amount of products in the waste stream by decomposition of phenolic resin. The temperature

of the process is 300-315 °C and the pressure is 200-250 kPa. The residence time is between 10 and 30 h (Zakoshansky 2007).

Aspen Plus was chosen for reactor simulation because Aspen Hysys has only a complicated Yield Shift Reactor that requires more input data than was found (Hamid 2007). In Aspen Plus Yield Reactor model can be used when stoichiometry of the reaction is unknown, when there is no information about reaction kinetics and there is only data about yield distribution (Al-Malah 2016). There is no data about the kinetics of reactions presented in Eq. 6-9. That is why it was decided to use the Yield Reactor to simulate the process. The inlet and outlet compositions of phenolic resin thermal cracking are presented in Table X.

Table X Phenolic resin decomposition with thermal cracking (Vol'-Epshtein, Gagarin 1973, Zakoshansky 2007).

Component	Inlet concentration, % mass	Outlet concentration, % mass
Ortho- and para- cumylphenol	42.4	13.0
AMS dimers	22.3	3.0
Acetophenone	12.7	12.8
Phenol	7.3	11.0
Dimethylphenylcarbinol	0.8	0.0
Polyalkylphenols and other products of deep condensation	12.4	24.6
Benzene	0.0	0.2
Toluene	0.0	0.7
Ethylbenzene	0.0	3.4
AMS	2.0	24.1
Cumene	0.1	7.2

Based concentrations in Table X the Yield Reactor model were filled. The NRTL method was again used as the estimation model, since it allows to simulate the non-ideal behavior in the liquid phase, and it is used for aqueous organics (Suppes 2002). NRTL is used for simulations related to cumene process (Andrigo, Caimi et al. 1992, Romanova, Leontiev 2015, Mafra,

Krähenbühl 2006, Cepeda, Gonzalez et al. 1989). The filled Yield Reactor model that was selected for simulations is shown in Figure 11.

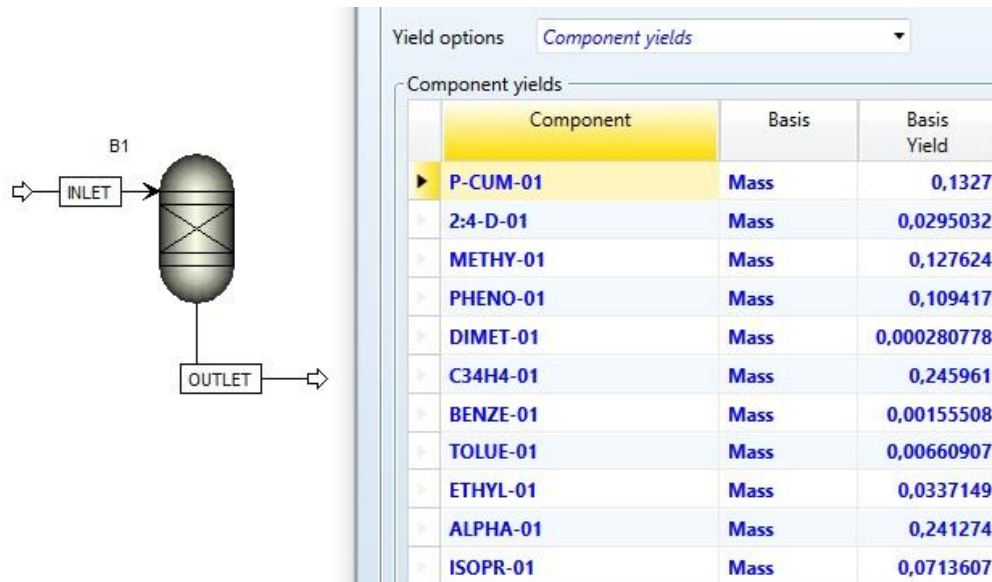


Figure 11 Reactor simulation in Aspen Plus

Phenolic resin has different composition at different plants, that is why it was decided to use typical phenolic resin composition as the inlet flow. The capacity of the reactor was selected based on typical waste stream amounts at a large-scale phenol production plant (Zakoshansky 2007). Mass balance of the simulation is shown in Table XI.

Table XI Thermal cracking reactor mass balance

Description	Phenolic resin	Decomposed phenolic resin
Para-Cumylphenol, kg/h	1963.8	614.4
AMS dimers, kg/h	1032.4	136.6
Acetophenone, kg/h	587.2	590.9
Phenol, kg/h	337.8	506.6
Dimethylphenylcarbinol, kg/h	37.9	1.3
AMS, kg/h	91.6	1117.1
Polyalkylphenols and other products of deep condensation, kg/h	574.6	1138.8
Benzene, kg/h	0.0	7.2
Toluene, kg/h	0.0	30.6
Ethylbenzene, kg/h	0.0	156.1
Cumene, Kg/h	4.7	330.4
Total, kg/h	4630.0	4630.0
Pressure, kPa	225.0	225.0
Temperature, °C	315.0	315.0

#### 5.4 Simulation of decomposed phenolic resin distillation: Aspen Hysys

Awareness of the boiling points of the substances helps to find a way of separation with minimal number of distillation columns. Boiling point of decomposed phenolic resin components can be found in Table XII.

Table XII Boiling points of decomposed phenolic resin components (Weast, Astle et al. 1988)

Component	Boiling point, °C
Benzene	80.1
Toluene	110.6
Ethylbenzene	136.4
Cumene	152.4
AMS	165.5
Phenol	181.9
Acetophenone	201.7
Dimethylphenylcarbinol	202.0
Para-Cumylphenol	335.0
AMS dimer	340.9

The inlet flow is made up of decomposed phenolic resin processed in the reactor of thermal cracking, and thus increases the content of the products in the stream. Based on the Table 5 it was decided to separate the unreacted phenolic resin with the phenol fraction from the mixture of light fraction with cumene and AMS in column D-6. The stream with phenolic resin and phenol fraction is sent back to the distillation stage of acetone and phenol to obtain commercial phenol. Thus, the yield of commercial phenol is increased. Column D-7 serves to separate the commercial product AMS as its boiling point is the lowest. Column D-8 serves to separate the light fractions from the commercial cumene. There was an option to use two columns instead of three adding lateral selection to the second column. However, since cumene and AMS have close boiling points, mutual spoiling takes place thus reducing commercial quality of these products. For these reasons it was decided to use three distillation columns, which would allow to separate the components at each stage in a way that each of them would have its highest boiling point. Thus, commercial product would be taken at the column bottom and have the minimal amount of impurities, which would meet commercial product requirements. The diagram of phenolic resin processing unit can be found in Figure 12.

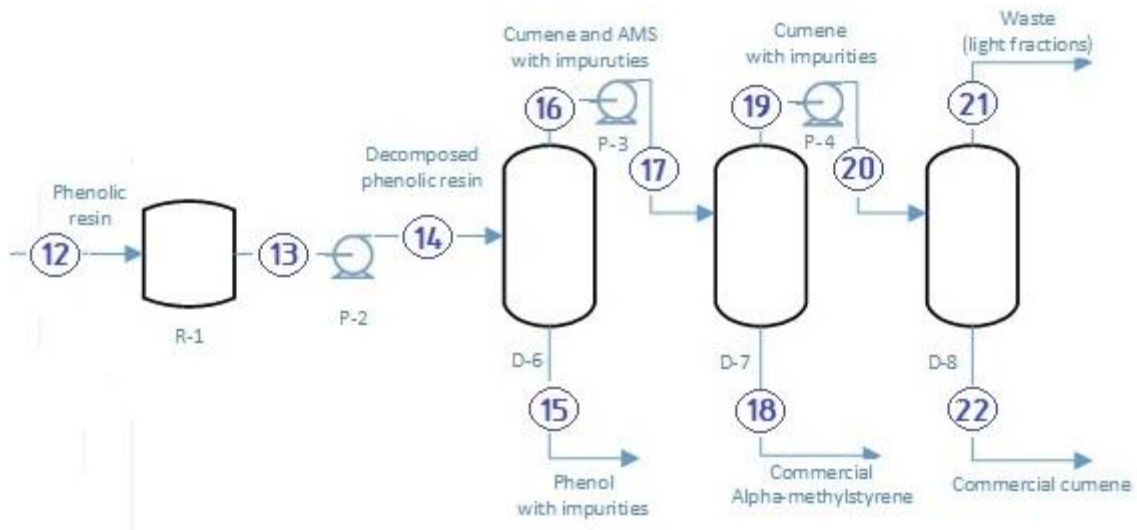


Figure 12 Diagram of phenolic resin processing unit

As in case of phenol and acetone distillation the NRTL method was chosen as the estimation model since it used for the similar components and serves to simulate the non-ideal behavior in the liquid phase (Suppes 2002). NRTL is used for simulations that are related to cumene process simulations (Andrigo, Caimi et al. 1992, Romanova, Leontiev 2015, Mafra, Krähenbühl 2006, Cepeda, Gonzalez et al. 1989). The inlet flow contains the decomposed phenolic resin after the reactor that was simulated in Aspen Plus. Simulation of the distillation scheme of phenolic resin processing unit in Aspen Hysys is presented in Figure 13.

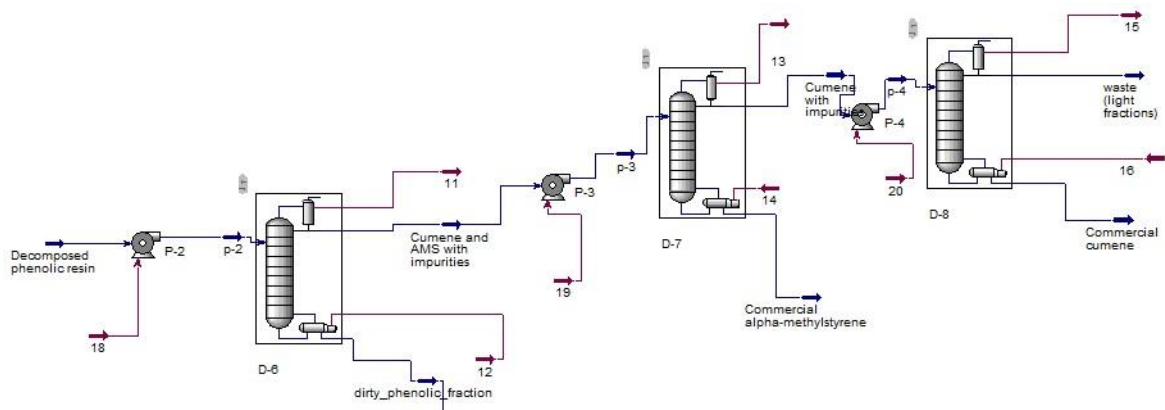


Figure 13 Simulation of phenolic resin processing unit distillation

The simulation part helps to find optimal parameters for distillation columns. The selection of the number of stages for column D-7 serves as an example and is shown in Figure 14, where graph represents the costs relation to reflux ratio divided by minimal reflux ratio. The diagram was drawn with fixed product concentration of commercial AMS. The costs were taken by Aspen Hysys Economics estimations.

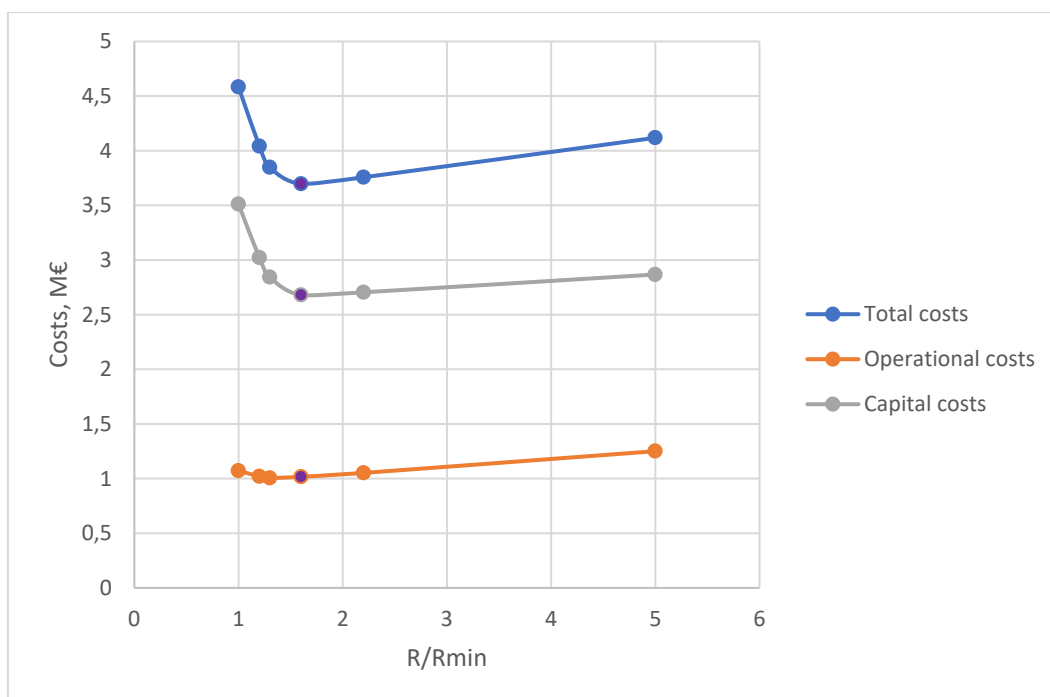


Figure 14 Diagram for choosing the number of stages and reflux ratio

Optimal column parameters are at the vertex of the total costs curve. Column with 50 stages and reflux ratio of 8 are optimal parameters for distillation that will provide low total costs. Similar diagrams were built for other distillation columns and optimal parameters were found. Column parameters are present in Table XIII. Mass balances of the distillation can be found in Table XIV.

Table XIII Distillation column parameters of phenolic resin processing unit

Column	D-6	D-7	D-8
Number of stages	40	50	40
Feed stage (top-down numbering)	28-36	30-38	6-14
Reflux ratio	35.0	8.0	37.0
Distillate rate	0.33	0.34	0.40
Pressure, kPa	10	40	100

Table XIV Mass balance for phenolic resin processing unit

	13	14	15	16	17
Description	Decomposed phenolic resin	(Pumped) Decomposed phenolic resin	Dirty phenolic fraction	Cumene and AMS with impurities	(Pumped) Cumene and AMS with impurities
Acetophenone, kg/h	590.9	590.9	590.9	0.0	0.0
Phenol, kg/h	506.6	506.6	506.6	0.0	0.0
Para-Cumylphenol, kg/h	614.4	614.4	614.4	0.0	0.0
AMS dimers, kg/h	1275.4	1275.4	1275.4	0.0	0.0
AMS, kg/h	1117.1	1117.1	110.9	1006.2	1006.2
Cumene, kg/h	330.4	330.4	0.4	330.0	330.0
Ethylbenzene, kg/h	156.1	156.1	0.1	156.0	156.0
Dimethylphenylcarbinol, kg/h	1.3	1.3	1.3	0.0	0.0
Benzene, kg/h	7.2	7.2	0.0	7.2	7.2
Toluene, kg/h	30.6	30.6	0.0	30.6	30.6
Total, kg/h	4630.0	4630.0	3100.0	1530.0	1530.0
Pressure, kPa	120.0	140.0	175.0	10.0	120.0
Temperature, °C	70.0	70.0	20.0	81.5	81.6

Table XIV (continued) Mass balance for phenolic resin processing unit

	18	19	20	21	22
Description	Commercial AMS	Cumene with impurities	(Pumped) Cumene with impurities	waste (light fractions)	Commercial cumene
Acetophenone, kg/h	0.0	0.0	0.0	0.0	0.0
Phenol, kg/h	0.0	0.0	0.0	0.0	0.0
Para-Cumylphenol, kg/h	0.0	0.0	0.0	0.0	0.0
AMS dimers, kg/h	0.0	0.0	0.0	0.0	0.0
AMS, kg/h	1005.9	0.3	0.3	0.0	0.3
Cumene, kg/h	7.1	322.9	322.9	13.2	309.7
Ethylbenzene, kg/h	0.0	156.0	156.0	156.0	0.0
Dimethylphenylcarbinol, kg/h	0.0	0.0	0.0	0.0	0.0
Benzene, kg/h	0.0	7.2	7.2	7.2	0.0
Toluene, kg/h	0.0	30.6	30.6	30.6	0.0
Total, kg/h	1013.0	517.0	517.0	207.0	310.0
Pressure, kPa	60.0	40.0	120.0	100.0	120.0
Temperature, °C	146.7	107.3	107.4	125.5	159.0

Heat flows for pinch analysis were obtained after the simulation. Energy balances of the distillation part of the phenolic resin processing unit can be found in Table XV. The numbering of heat flows was given in Figure 13.

Table XV Energy balance for phenolic resin processing unit

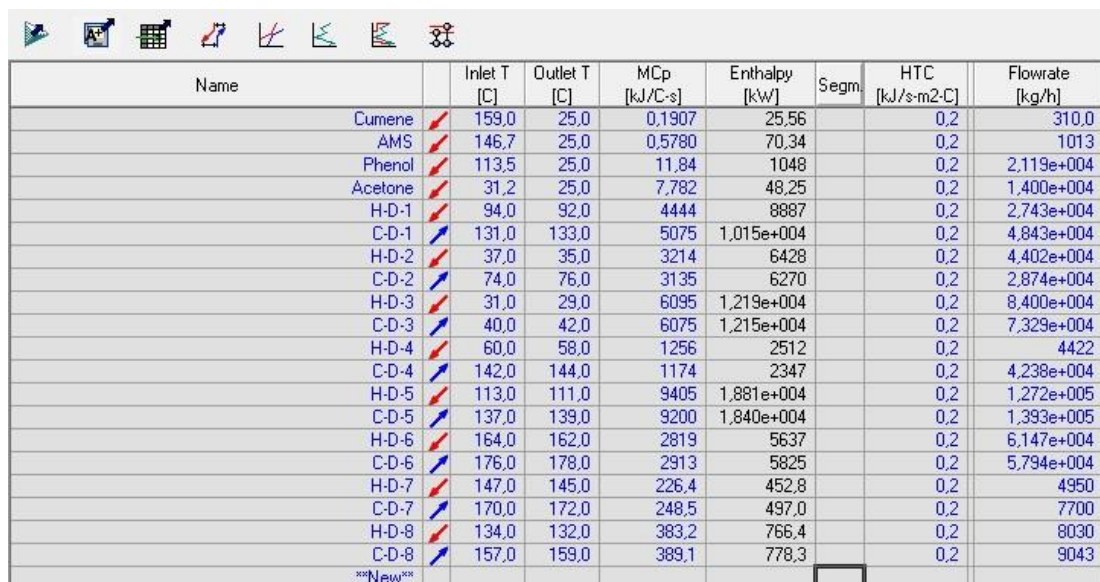
		Heat flow, kJ/h	Power, kW
D-6	11	$2.03 \cdot 10^7$	5637.0
	12	$2.10 \cdot 10^7$	5825.0
D-5	13	$1.63 \cdot 10^6$	452.8
	14	$1.79 \cdot 10^6$	497.0
D-7	15	$2.76 \cdot 10^6$	766.4
	16	$2.80 \cdot 10^6$	778.3

## 6 Pinch analysis

In order to satisfy the cooling, heating and power demands of a process it is preferable to design a network of heat exchangers (HEN) that enables the minimum usage of utilities. The main idea of HENs is the efficient energy utilization in the hot process streams to heat cold process streams. For this reason, the maximum energy recovery (MER) is usually calculated to define the minimum hot and cold utilities in the network, considering the heating and cooling requirements of the process streams. The term “MER targeting” is usually used for the process. There are three methods used to determine MER targets, namely 1) the temperature-interval method, 2) a graphical method with composite heating and cooling curves and 3) the creation and solving a linear programming model (Seider, Seader et al. 2010).

In this paper the graphical composite curve method was used, since the graphical display of Aspen Energy Analyzer gives the opportunity to clearly understand the notion of pinch which is the point of closest approach between the hot and cold composite curves. The design started at the found pinch point gives the opportunity to meet the energy targets using HENs that recover heat between hot and cold streams in two separate systems, one for temperatures above pinch temperatures and one for temperatures below pinch temperatures.

Aspen Energy Analyzer was chosen for pinch analysis. Heat flow parameters that are presented in Figure 15 were collected after simulations in Aspen Hysys. High pressure steam and cooling water were chosen as utility streams.



Name	Inlet T [C]	Outlet T [C]	MCp [kJ/C-s]	Enthalpy [kW]	Segm	HTC [kJ/s-m2-C]	Flowrate [kg/h]
Cumene	159,0	25,0	0,1907	25,56		0,2	310,0
AMS	146,7	25,0	0,5780	70,34		0,2	1013
Phenol	113,5	25,0	11,84	1048		0,2	2,119e+004
Acetone	31,2	25,0	7,782	48,25		0,2	1,400e+004
H-D-1	94,0	92,0	4444	8887		0,2	2,743e+004
C-D-1	131,0	133,0	5075	1,015e+004		0,2	4,843e+004
H-D-2	37,0	35,0	3214	6428		0,2	4,402e+004
C-D-2	74,0	76,0	3135	6270		0,2	2,874e+004
H-D-3	31,0	29,0	6095	1,219e+004		0,2	8,400e+004
C-D-3	40,0	42,0	6075	1,215e+004		0,2	7,329e+004
H-D-4	60,0	58,0	1256	2512		0,2	4422
C-D-4	142,0	144,0	1174	2347		0,2	4,238e+004
H-D-5	113,0	111,0	9405	1,881e+004		0,2	1,272e+005
C-D-5	137,0	139,0	9200	1,840e+004		0,2	1,393e+005
H-D-6	164,0	162,0	2819	5637		0,2	6,147e+004
C-D-6	176,0	178,0	2913	5825		0,2	5,794e+004
H-D-7	147,0	145,0	226,4	452,8		0,2	4950
C-D-7	170,0	172,0	248,5	497,0		0,2	7700
H-D-8	134,0	132,0	383,2	766,4		0,2	8030
C-D-8	157,0	159,0	389,1	778,3		0,2	9043
***New**							

Figure 15 Inlet data for pinch analysis. H – hot stream, C – cold stream, D – column



## 7 Equipment sizing

Equipment sizing is an essential part of the capital costs estimation. In this part distillation columns, reactor, heat exchangers and pumps sizing were calculated.

### 7.1 Distillation columns sizing

Vessel mass and the number of trays with their types are required to estimate distillation columns costs. Columns D-6 and D-7 operate under vacuum pressure, that is why it was decided to use sieve trays for them. Column D-8 operates under atmospheric pressure, that is why it was decided to use valve trays for it (Couper, Penney et al. 2012). An example of a valve tray calculation for column D-8 can be found in Appendix I. An example of vessel mass calculation for column D-8 is presented in Appendix II. Sizing results can be found in Table XVII.

Table XVII Distillation column sizing parameters

Column	D-6	D-7	D-8
Type of contact devices	Sieve trays	Sieve trays	Valve trays
Number of trays	60	70	50
Tray diameter, m	2.4	0.8	1.8
Column height, m	30	35	25
Vessel mass, t	23.3	4.3	4.8

### 7.2 Reactor sizing

Residence time for thermal cracking of phenolic resin is 10-30 h (Zakoshansky 2007). For calculations 20 h was taken as the residence time. Reactor vessel volume was calculated based on residence time and flow rate:

$$V_R = F_R \cdot T \quad (10)$$

where  $V_R$  is reactor vessel volume,  $F_R$  is reactor flow rate,  $T$  is residence time.

$$V_R = 4.2 \cdot 20 = 84 \text{ m}^3$$

### 7.3 Heat exchangers sizing

Heat exchangers were calculated by using Aspen Energy Analyzer. Results for two systems can be found in Table XVIII. Heat exchanger E-21 was also calculated by using Aspen Energy Analyzer, it is similar for both systems since pinch analysis was done only for distillation columns.

Table XVIII Heat exchangers for system with and without HEN

With HEN		Without HEN	
Heat exchanger	Area, m <sup>2</sup>	Heat exchanger	Area, m <sup>2</sup>
E-1	325.6	E-1	325.1
E-2	56.2	E-2	275.2
E-3	35.9	E-3	35.9
E-4	26.0	E-4	26.0
E-5	382.8	E-5	382.0
E-6	4.7	E-6	166.5
E-7	95.6	E-7	95.6
E-8	730.3	E-8	727.4
E-9	14.2	E-9	32.9
E-10	6.7	E-10	14.2
E-11	1070.4	E-11	598.6
E-12	122.3	E-12	6.7
E-13	277.0	E-13	1080.6
E-14	4874.5	E-14	122.4
E-15	2.3	E-15	197.9
E-16	1490.3	E-16	277.6
E-17	82.8	E-17	5169.3
E-18	63.0	E-18	17.6
E-19	1718.2	E-19	2.3
E-20	641.3	E-20	1510.8
E-21	179.1	E-21	179.1

#### 7.4 Pumps sizing

Pumps were calculated by using Aspen Hysys. Results can be found in Table XIX.

Table XIX Calculated pump parameters

	Pump type	Parameters
P-1	Centrifugal pump	Volume flow rate 5.31 m <sup>3</sup> /h Pump power 270 W
P-2	Liquid-ring pump	Volume flow rate 5.38 m <sup>3</sup> /h Pump power 36 W
P-3	Centrifugal pump	Volume flow rate 2.00 m <sup>3</sup> /h Pump power 74 W
P-4	Centrifugal pump	Volume flow rate 0.72 m <sup>3</sup> /h Pump power 20 W

## 8 Economic evaluation

Economic evaluation of the project will be the answer to the question of its profitability. Capital and operational costs and the project revenue were calculated to estimate economic potential of the project. Costs comparison for systems with and without HEN is also given in this chapter.

### 8.1 Capital costs

Capital costs of phenolic resin processing unit which includes one reactor, three distillation columns, ten heat exchangers and four pumps were calculated based on the Eq. 11 (Towler, Sinnott 2012).

$$C_p = a + b \cdot Y^u \quad (11)$$

where  $C_p$  is calculated equipment price,  $a$  is first cost constant,  $b$  is second cost constant,  $Y$  is size parameter,  $u$  is exponent for type of equipment.

Example of price calculation for reactor with volume as a size parameter:

$$C_p = 61500 + 32500 \cdot 84^{0.8} = 1.19 \text{ M\$}$$

Costs are not static because of inflation, that is why they commonly increase with time. Chemical engineering plant cost index (CEPCI) was used to get actual price in 2018 by using Eq. 12. CEPCI is 532.9 for reactor, distillation columns, heat exchangers and pumps, as prices for calculation were given for the year 2010 (Towler, Sinnott 2012).

$$C_{p2018} = C_{p2010} \cdot \frac{CEPCI_{2018}}{CEPCI_{2010}} \quad (12)$$

where  $C_{p2018}$  is calculated equipment price for the year 2018,  $C_{p2010}$  is calculated equipment price for the year 2010,  $CEPCI_{2018}$  is chemical engineering plant cost index for the year 2018,  $CEPCI_{2010}$  is chemical engineering plant cost index for the year 2010.

An example of reactor price calculation for the year 2018, where CEPCI is 603.1 for the year 2018 (Chemical engineering 2019), is given below:

$$C_{p2018} = 1.2 \cdot \frac{603.1}{532.9} = 1.35 \text{ M\$}$$

Installation factor helps to get installed equipment price, which is calculated by Eq. 13. Installation factor is 4 for distillation columns, 3.5 for heat exchangers, 4 for pressure vessels and 4 for pumps (Towler, Sinnott 2012).

$$C_{pinst} = C_p \cdot F_{inst} \quad (13)$$

where  $C_{pinst}$  is installed equipment price,  $F_{inst}$  is installation factor.

An example of cost calculation for installed reactor is the following:

$$C_{pinst} = 1.35 \cdot 4 = 5.4 \text{ M\$}$$

Coefficient that was used for \$ conversion into € is 0.88 (Transferwise 2019) and final cost for installed reactor is 4.75 M€. Installed factor, CEPCI for 2018 and currency conversion were used for all equipment.

Before calculating capital costs, it is necessary to decide whether to use created HEN or not. Prices for heat exchangers from Table X were calculated by using heat exchanger area as a size parameter. Costs for utilities from Table VIII were calculated with 0.3 €/m<sup>3</sup> for cooling water and 0.015 €/kg for high pressure steam (Seider, Seader et al. 2010). Calculated prices can be found in Table XX.

Table XX Costs for system with and without HEN

	With HEN	Without HEN
High pressure steam, M€/year	11.25	15.61
Cooling water, M€/year	18.53	25.63
Heat exchangers, M€	12.20	11.40

Costs difference for heat exchangers is only 0.8 M€, while costs difference for utilities is 11.46 M€/year. That is why it is better to use created HEN as it will help to save money. Thus, heat exchangers of phenolic resin processing unit, that will be given further, are calculated with consideration of this fact. The results of capital costs calculation can be found in Table XXI.

Table XXI Project capital costs

Equipment	Specification	Equipment price, M€	Reference	Price basis
Reactor	Thermal cracking reactor: volume 84 m <sup>3</sup>	4.75	(Towler, Sinnott 2012)	Reactor price was calculated considering its volume as a size parameter.
Distillation columns	Column D-6: sieve trays, diameter 2.4 m, height 30 m, mass 23.3 t Column D-7: sieve trays, diameter 0.8 m, height 35 m, mass 4.3 t Column D-8: valve trays, diameter 1.8 m, height 25 m, mass 4.8 t	1.86	(Towler, Sinnott 2012)	Distillation column prices were calculated by combining vessel and trays prices.
Heat exchangers	Heat exchangers: E-1: area 325.6 m <sup>2</sup> E-3: area 35.6 m <sup>2</sup> E-4: area 26 m <sup>2</sup> E-10: area 6.7 m <sup>2</sup> E-12: area 122.3 m <sup>2</sup> E-15: area 2.3 m <sup>2</sup> E-17: area 82.8 m <sup>2</sup> E-18: area 63 m <sup>2</sup> E-20: area 641.3 m <sup>2</sup> E-21: area 171.9 m <sup>2</sup>	1.67 M€	(Towler, Sinnott 2012)	Heat exchanger prices were calculated considering heat exchanger area as a size parameter.
Pumps	Centrifugal pump P-1: volume flow rate 5.31 m <sup>3</sup> /h, pump power 270 W Liquid-ring pump P-2: volume flow rate 5.38 m <sup>3</sup> /h, pump power 36 W Centrifugal pump P-3: volume flow rate 2.00 m <sup>3</sup> /h, pump power 74 W Centrifugal pump P-4: volume flow rate 0.72 m <sup>3</sup> /h, pump power 20 W	0.15 M€	(Seider, Seader et al. 2010)	Pump prices were calculated considering volume flow rates as a size parameter
Total equipment costs		8.43		

The equivalent annual costs (EAC) was calculated by Eq. 14 with internal rate of return (IRR) of 10 % in 15 years (Max, Klaus et al. 1991).

$$EAC = \frac{\text{total equipment costs} \cdot IRR}{1 - (1 - IRR)^{time}} \quad (14)$$

where  $EAC$  is equivalent annual costs,  $IRR$  is internal rate of return.

$$EAC = \frac{8.43 \cdot 10^6 \cdot 0.1}{1 - (1 - 0.1)^{15}} = 1.06 \text{ M€}/\text{year}$$

## 8.2 Operational costs

Heating of the reactor by natural gas was calculated by Aspen Energy Analyser. Electricity consumption was calculated by using Aspen Hysys and Aspen Plus. Consumption of high pressure steam and cooling water was calculated with Aspen Energy Analyser. Since it was decided to use HEN, annual cooling water consumption turned out to be low, because top column streams of phenolic resin processing unit are cooled down by heating the bottom of acetone separation columns, as it was showed in Figure 16. Index for the year 2018 was used to get actual utility prices. The results of operational costs calculation are presented in Table XXII.

Table XXII Project operational costs (Seider, Seader et al. 2010)

	Annual consumption	Cost, M€
High pressure steam	0.23 Mt	3.48
Cooling water	$25.7 \cdot 10^3 \text{ m}^3$	$7.7 \cdot 10^{-3}$
Natural gas	2984 t	1.93
Electricity	2102 MWh	0.124
Total operational costs		5.55

## 8.3 Economic potential

Revenue was calculated by using product prices form Table V. Results of the revenue calculation are presented in Table XXIII.

Table XXIII Project revenue

	Annual production, t	Cost, M€
Phenol	4380	4.25
AMS	8760	6.13
Cumene	2715.6	3.59
Total revenue		13.97

The economic potential of the project was calculated by Eq. 15 (Max, Klaus et al. 1991).

$$\text{Economic potential} = \text{Revenue} - \text{Operational costs} - \text{EAC} \quad (15)$$

$$\text{Economic potential} = 13.97 - 5.55 - 1.06 = 7.36 \text{ M€}/\text{year}$$

Phenolic resin processing unit proved to be profitable enough with economic potential of 7.36 M€/year.

## Conclusion

The main goal of this thesis was to develop the equipment and technology for phenolic resin processing unit used at phenol production by cumene process. It was crucial to ensure profitability of the technology and sustainability of the unit, as well as to reduce adverse environmental impact from production. According to the results obtained in the simulations, the reduction in the amount of waste products, namely phenolic resin discussed in this thesis, by 61 % was achieved, thus increasing sustainability of the process.

As of the process profitability, the goal was achieved to some extent. In the literature part a few modern methods of phenol production were discussed. Based on the analysis of the methods the cumene method proved to be the most efficient one from the economic point of view, with 97 % mol selectivity. What is more, the research showed that this method is widely used at phenol and acetone production plants throughout the world. For these reasons the cumene method seems to be predominant in the industry for years to come. Since phenol production by the cumene method has phenolic resin as its hazardous waste product, the issue of phenolic resin processing is also a poignant one. In the literature part several methods of phenolic resin processing were given view of. The process of thermal cracking came to be the most profitable, because of its ability to extract the useful products contained in phenolic resin. The process of potentially profitable catalytic cracking discussed in the literature part did not prove to be as efficient and profitable as the thermal one, as it spoils phenolic fraction recycle flow which is, if untreated, spoils commercial phenol. Thus, thermal cracking was chosen as a preferable option for phenolic resin processing. The research showed that thermal cracking encourages the production of cumene, as well as the increase in phenol and AMS contained in phenolic resin.

The analysis of boiling points of decomposed phenolic resin components in the experimental part allowed to opt for a three distillation columns layout to separate phenolic fraction with the unreacted phenolic resin, AMS and commercial cumene. Since phenolic resin has different composition at different plants, a typical phenolic resin composition as taken as well as typical capacity for phenol production, namely 200000 t/year of phenol and 125000 t/year of acetone. As a result, the 310 kg/h of commercial cumene and 1000 kg/h of AMS were obtained, with commercial phenol yield being increased by 500 kg/h.

Apart from that, pinch analysis of the heat flows of phenol and acetone separation part and phenolic resin processing unit separation part was done. As a result, HEN was created, which allowed to reduce utility costs. Equipment sizing was done for capital costs calculation where IRR is taken as

10 % in 15 years. Operational costs and revenue were calculated for economic evaluation of the project. Phenolic resin processing unit proved to be profitable enough with economic potential of 7.36 M€/year. Thus, the results obtained in this Master's thesis allow to consider the designed phenolic resin processing unit suitable for phenol and acetone production plants by cumene method, with its implementation encouraging profitability and sustainability of production.

## REFERENCES

- Advansix, 2018-last update, Alpha-methylstyrene – product specifications. Available: <https://www.advansix.com/chemicalintermediates/?document=alpha-methylstyrene-ams&download=1> [May 16, 2019].
- Al-Malah, K.I., 2016. *Aspen plus: chemical engineering applications*. John Wiley & Sons.
- Altivia, 2015-last update, Phenol - Product Data Sheet – typical properties and specifications. Available: [http://altiviatest.com/Resources/TDS/ALTIVIA\\_Phenol\\_Data\\_Sheet.pdf](http://altiviatest.com/Resources/TDS/ALTIVIA_Phenol_Data_Sheet.pdf) [May 16, 2019].
- Andrigo, P., Caimi, A., d'Oro, P.C., Fait, A., Roberti, L., Tampieri, M. and Tartari, V., 1992. Phenol-acetone process: cumene oxidation kinetics and industrial plant simulation. *Chemical engineering science*, 47(9-11), pp.2511-2516.
- Bahramian, A.R., Kokabi, M., Famili, M.H.N. and Beheshty, M.H., 2006. Ablation and thermal degradation behaviour of a composite based on resol type phenolic resin: process modeling and experimental. *Polymer*, 47(10), pp.3661-3673.
- Balducci, L., Bianchi, D., Bortolo, R., D'Aloisio, R., Ricci, M., Tassinari, R. and Ungarelli, R., 2003. Direct oxidation of benzene to phenol with hydrogen peroxide over a modified titanium silicalite. *Angewandte Chemie International Edition*, 42(40), pp.4937-4940.
- Bender, H.L., Farnham, A.G., Guyer, J.W., Apel, F.N. and Gibb, T.B., 1952. Purified chemicals and resins from Phenol and Formaldehyde. *Industrial & Engineering Chemistry*, 44(7), pp.1619-1623.
- Borealis, 2019-last update, Phenol & Acetone. Available: <https://www.borealisgroup.com/base-chemicals/hydrocarbons-energy/phenol-acetone> [May 25, 2019].
- Burch, R. and Howitt, C., 1992. Direct partial oxidation of benzene to phenol on zeolite catalysts. *Applied Catalysis A: General*, 86(2), pp.139-146.
- Busca, G., Berardinelli, S., Resini, C. and Arrighi, L., 2008. Technologies for the removal of phenol from fluid streams: a short review of recent developments. *Journal of hazardous materials*, 160(2-3), pp.265-288.

Cepeda, E., Gonzalez, C. and Resa, J.M., 1989. Isobaric vapor-liquid equilibrium for the cumene-phenol system. *Journal of Chemical and Engineering Data*, 34(3), pp.270-273.

Couper, J.R., Penney, W.R. and Fair, J.R., 2012. *Chemical Process Equipment-Selection and Design (Revised 3rd Edition)*. Butterworth-Heinemann.

Chemical engineering, 2019-last update, Chemical engineering plant cost index: 2018 annual value. Available: <https://www.chemengonline.com/2019-cepci-updates-january-prelim-and-december-2018-final/> [May 25, 2019].

Cheng, J.C.Y., Buchanan, J.S., Levin, D., Steckel, M.A., Dakka, J.M., Stokes, J.P., Robbins, J.L., Stanat, J.E., Smith, C.M. and Santiesteban, J.G., ExxonMobil Chemical Patents Inc, 2010. *Process for producing phenol and methyl ethyl ketone*. U.S. Patent 7,799,956.

Chianese, A., 1982. A mathematical model of a bubble column reactor for the cumene oxidation. *Chemical Engineering Communications*, 17(1-6), pp.261-271.

Chudinova, A., Salischeva, A., Ivashkina, E., Moizes, O. and Gavrikov, A., 2015. Application of cumene technology mathematical model. *Procedia Chemistry*, 15, pp.326-334.

Colonial, 2019-last update, Sales Specifications – Acetone. Available: [http://colonialchemicals.com/uploads/Products/Acetone/Acetone\\_Tech.pdf](http://colonialchemicals.com/uploads/Products/Acetone/Acetone_Tech.pdf) [May 16, 2019].

Correia, P.F. and de Carvalho, J.M., 2003. Recovery of phenol from phenolic resin plant effluents by emulsion liquid membranes. *Journal of Membrane Science*, 225(1-2), pp.41-49.

Dakka, J.M., Levin, D., Buchanan, J.S. and Stanat, J.E.R., ExxonMobil Chemical Patents Inc, 2008. *Process for oxidizing alkylaromatic compounds*. U.S. Patent 7,446,232.

Di Somma, I., Andreozzi, R., Canterino, M., Caprio, V. and Sanchirico, R., 2008. Thermal decomposition of cumene hydroperoxide: chemical and kinetic characterization. *AIChE journal*, 54(6), pp.1579-1584.

Dow, 2013-last update, Cumene – product specifications. Available: [http://msdssearch.dow.com/PublishedLiteratureDOWCOM/dh\\_08cd/0901b803808cd61e.pdf?filepath=aromatics/pdfs/noreg/778-04601.pdf&fromPage=GetDoc](http://msdssearch.dow.com/PublishedLiteratureDOWCOM/dh_08cd/0901b803808cd61e.pdf?filepath=aromatics/pdfs/noreg/778-04601.pdf&fromPage=GetDoc) [May 16, 2019].

Fathi-Afshar, S. and Rudd, D.F., 1981. The economic impact of new chemical technology. *Chemical Engineering Science*, 36(8), pp.1421-1425.

Fellah, M.F., van Santen, R.A. and Onal, I., 2009. Oxidation of benzene to phenol by N<sub>2</sub>O on an Fe<sup>2+</sup>-ZSM-5 cluster: A density functional theory study. *The Journal of Physical Chemistry C*, 113(34), pp.15307-15313.

Gardziella, A., Pilato, L.A. and Knop, A., 2013. *Phenolic resins: chemistry, applications, standardization, safety and ecology*. Springer Science & Business Media.

Gera, V., Panahi, M., Skogestad, S. and Kaistha, N., 2012. Economic plantwide control of the cumene process. *Industrial & Engineering Chemistry Research*, 52(2), pp.830-846.

Gopalakrishnan, S., Münch, J., Herrmann, R. and Schwieger, W., 2006. Effects of microwave radiation on one-step oxidation of benzene to phenol with nitrous oxide over Fe-ZSM-5 catalyst. *Chemical Engineering Journal*, 120(1-2), pp.99-105.

Grbić-Galić, D. and Vogel, T.M., 1987. Transformation of toluene and benzene by mixed methanogenic cultures. *Appl. Environ. Microbiol.*, 53(2), pp.254-260.

Hamid, M.K.A., 2007. HYSYS: An Introduction to Chemical Engineering Simulation. *Apostila de Hamid*.

Hensen, E.J.M., Zhu, Q., Janssen, R.A.J., Magusin, P.C.M.M., Kooyman, P.J. and Van Santen, R.A., 2005. Selective oxidation of benzene to phenol with nitrous oxide over MFI zeolites: 1. On the role of iron and aluminum. *Journal of Catalysis*, 233(1), pp.123-135.

Hensen, E., Zhu, Q., Liu, P.H., Chao, K.J. and van Santen, R., 2004. On the role of aluminum in the selective oxidation of benzene to phenol by nitrous oxide over iron-containing MFI zeolites: an in situ Fe XANES study. *Journal of catalysis*, 226(2), pp.466-470.

Hiemer, U., Klemm, E., Scheffler, F., Selvam, T., Schwieger, W. and Emig, G., 2004. Microreaction engineering studies of the hydroxylation of benzene with nitrous oxide. *Chemical Engineering Journal*, 101(1-3), pp.17-22.

ICIS, 2010-last update, Alpha-methylstyrene. Available: <https://www.icis.com/explore/resources/news/2000/05/22/115657/Alpha-methylstyrene/> [May 18, 2019].

ICIS, 2016-last update, OUTLOOK '17: Asia phenol may surprise to the upside. Available: <https://www.icis.com/explore/resources/news/2016/12/28/10061834/outlook-17-asia-phenol-may-surprise-to-the-upside/> [May 25, 2019].

ICIS, 2012-last update, US April cumene prices assessed at rollover on feedstocks. Available: <https://www.icis.com/explore/resources/news/2012/04/06/9548399/us-april-cumene-prices-assessed-at-rollover-on-feedstocks/> [May 18, 2019].

Industry standard, 1983. *Apparaty kolonnye tarel'chatye, metod tekhnologicheskogo i gidrodinamicheskogo rascheta [Tray-type column, method of technological and hydrodynamic calculation]*. [In Russian]

INEOS Phenol, 2019-last update, Antwerp, Belgium. Available: <https://www.ineos.com/businesses/ineos-phenol/sites/> [May 25, 2019].

Intratec, 2019-last update, Cumene – Price History & Forecast. Available: <https://www.intratec.us/chemical-markets/cumene-price> [May 16, 2019].

Intratec, 2019-last update, Phenol – Price History & Forecast. Available: <https://www.intratec.us/chemical-markets/phenol-price> [May 16, 2019].

Kachurovskaya, N.A., Zhidomirov, G.M. and van Santen, R.A., 2004. Computational study of benzene-to-phenol oxidation catalyzed by N<sub>2</sub>O on iron-exchanged ferrierite. *The Journal of Physical Chemistry B*, 108(19), pp.5944-5950.

Knop, A. and Pilato, L.A., 2013. *Phenolic resins: chemistry, applications and performance*. Springer Science & Business Media.

Kujawski, W., Warszawski, A., Ratajczak, W., Porebski, T., Capała, W. and Ostrowska, I., 2004. Removal of phenol from wastewater by different separation techniques. *Desalination*, 163(1-3), pp.287-296.

Levin, M.E., Gonzales, N.O., Zimmerman, L.W. and Yang, J., 2006. Kinetics of acid-catalyzed cleavage of cumene hydroperoxide. *Journal of hazardous materials*, 130(1-2), pp.88-106.

Leanza, R., Rossetti, I., Mazzola, I. and Forni, L., 2001. Study of Fe-silicalite catalyst for the N<sub>2</sub>O oxidation of benzene to phenol. *Applied Catalysis A: General*, 205(1-2), pp.93-99.

Leontiev, V.S. and Romanova, N.A., 2015. Hardware and process optimization of production unit for concentrating isopropyl benzene hydroperoxide in the course of phenol production by cumene process. *Oil & Gas Business*, (3).

Levchik, S.V. and Weil, E.D., 2004. Thermal decomposition, combustion and flame-retardancy of epoxy resins—a review of the recent literature. *Polymer International*, 53(12), pp.1901-1929.

- Liu, Y., Lu, Y., Liu, P., Gao, R. and Yin, Y., 1998. Effects of microwaves on selective oxidation of toluene to benzoic acid over a  $V_2O_5/TiO_2$  system. *Applied Catalysis A: General*, 170(2), pp.207-214.
- Liu, Y., Murata, K. and Inaba, M., 2006. Direct oxidation of benzene to phenol by molecular oxygen over catalytic systems containing Pd (OAc) 2 and heteropolyacid immobilized on HMS or PIM. *Journal of Molecular Catalysis A: Chemical*, 256(1-2), pp.247-255.
- Li, Y., Feng, Z., Van Santen, R.A., Hensen, E.J.M. and Li, C., 2008. Surface functionalization of SBA-15-ordered mesoporous silicas: Oxidation of benzene to phenol by nitrous oxide. *Journal of Catalysis*, 255(2), pp.190-196.
- Loos, A.C. ed., 2000. *Processing of composites* (p. 320). Munich: Hanser Publishers.
- Luyben, William L. "Design and control of the cumene process." *Industrial & Engineering Chemistry Research* 49, no. 2 (2009): 719-734.
- Mafra, M.R. and Krähenbühl, M.A., 2006. Liquid– liquid equilibrium of (water+ acetone) with cumene or  $\alpha$ -methylstyrene or phenol at temperatures of (323.15 and 333.15) K. *Journal of Chemical & Engineering Data*, 51(2), pp.753-756.
- Marketsinsider, 2019-last update, Global Phenol Market Report 2017-2021. Available: <https://markets.businessinsider.com/news/stocks/global-phenol-market-report-2017-2021-featuring-ineos-group-mitsui-chemicals-ptt-global-chemical-royal-dutch-shell-solvay-1003202598> [May 16, 2019].
- Matar, S. and Hatch, L.F., 2001. *Chemistry of petrochemical processes*. Elsevier.
- Matsui, S. and Fujita, T., 2001. New cumene-oxidation systems:  $O_2$  activator effects and radical stabilizer effects. *Catalysis today*, 71(1-2), pp.145-152.
- Max, S.P., Klaus, D.T. and Ronald, E.W., 1991. Plant design and economics for chemical engineers. *International edition*.
- Meikrantz, D.H., Bourne, G.L., McFee, J.N., Burdge, B.G. and McConnell Jr, J.W., US Department of Energy, 1991. *Method of recovering hazardous waste from phenolic resin filters*. U.S. Patent 4,995,916.

Meloni, D., Monaci, R., Solinas, V., Berlier, G., Bordiga, S., Rossetti, I., Oliva, C. and Forni, L., 2003. Activity and deactivation of Fe-MFI catalysts for benzene hydroxylation to phenol by  $N_2O$ . *Journal of Catalysis*, 214(2), pp.169-178.

McKetta Jr, J.J. ed., 1990. *Encyclopedia of Chemical Processing and Design: Volume 35- Petroleum Fractions Properties to Phosphoric Acid Plants: Alloy Selection*. CRC press.

Nexant Chem Systems, 2006. Phenol/MEK Co-Product Process.

Notté, P.P., 2000. The AlphOx TM process or the one-step hydroxylation of benzene into phenol by nitrous oxide. Understanding and tuning the ZSM-5 catalyst activities. *Topics in catalysis*, 13(4), pp.387-394.

Ohkubo, K., Kobayashi, T. and Fukuzumi, S., 2011. Direct oxygenation of benzene to phenol using quinolinium ions as homogeneous photocatalysts. *Angewandte Chemie International Edition*, 50(37), pp.8652-8655.

Palma, M.S.A., Paiva, J.L.D., Zilli, M. and Converti, A., 2007. Batch phenol removal from methyl isobutyl ketone by liquid-liquid extraction with chemical reaction. *Chemical Engineering and Processing: Process Intensification*, 46(8), pp.764-768.

Parmon, V.N., Panov, G.I., Uriarte, A. and Noskov, A.S., 2005. Nitrous oxide in oxidation chemistry and catalysis: application and production. *Catalysis Today*, 100(1-2), pp.115-131.

Pirutko, L.V., Uriarte, A.K., Chernyavsky, V.S., Kharitonov, A.S. and Panov, G.I., 2001. Preparation and catalytic study of metal modified TS-1 in the oxidation of benzene to phenol by  $N_2O$ . *Microporous and mesoporous materials*, 48(1-3), pp.345-353.

Pilato, L. ed., 2010. *Phenolic resins: a century of progress*(Vol. 11, p. 2010). New York: Springer.

Pillai, K.S., Jia, J. and Sachtler, W.M., 2004. Effect of steaming on one-step oxidation of benzene to phenol with nitrous oxide over Fe/MFI catalysts. *Applied Catalysis A: General*, 264(2), pp.133-139.

Pland, 2015-last update, Stainless steel sheet thickness. Available: <http://www.plandstainless.co.uk/sheet-thickness/> [May 12, 2019].

Rappoport, Z., 2004. *The chemistry of phenols*. John Wiley & Sons.

Ren, T., Yan, L., Zhang, X. and Suo, J., 2003. Selective oxidation of benzene to phenol with  $N_2O$  by unsupported and supported  $FePO_4$  catalysts. *Applied Catalysis A: General*, 244(1), pp.11-17.

- Revie, R.W. ed., 2011. *Uhlig's corrosion handbook* (Vol. 57). John Wiley & Sons.
- Romanova, N.A. and Leontiev, V.S., 2017. Structure and energy optimization of the phenol and acetone separation process using reaction mixture components as entrainers. *Petroleum Chemistry*, 57(5), pp.430-435.
- Sassda, 2017-last update, The mechanical properties of stainless steel. Available: <http://nssc.co.za/wp-content/uploads/2017/03/info-series-no-3-mechanical-properties-of-stainless-steel.pdf> [May 25, 2019].
- Schmidt, R.J., 2005. Industrial catalytic processes—phenol production. *Applied Catalysis A: General*, 280(1), pp.89-103.
- Seider, W.D., Seader, J.D. and Lewin, D.R., 2010. *Product & Process Design Principles: Synthesis, Analysis and Evaluation, (With CD)*. John Wiley & Sons.
- Suppes, G.J., 2002. Selecting thermodynamic models for process simulation of organic VLE and LLE systems. *ChapterONE Online* (2002).
- Taboada, J.B., 2006. *Direct Oxidation of Benzene to Phenol: investigation of the active iron species in [Fe, Al] MFI catalysts by <sup>57</sup>Fe Mössbauer spectroscopy*. IOS Press.
- The Physics Factbook, 2019-last update, Density of steel. Available: <https://hypertextbook.com/facts/2004/KarenSutherland.shtml> [May 25, 2019].
- Timonin, A.S., 2002. *Osnovy konstruirovaniya i rascheta himiko-tekhnologicheskogo i prirodoohrannogo oborudovaniya [Fundamentals of design and calculation of chemical-technological and environmental equipment]*. Directory. Volume 2. [In Russian]
- Towler, G. and Sinnott, R., 2012. *Chemical engineering design: principles, practice and economics of plant and process design*. Elsevier.
- Transferwise, 2019-last update, USD to EUR converter. Available: <https://transferwise.com/gb/currency-converter/usd-to-eur-rate> [May 16, 2019].
- Tzeng, S.S. and Chr, Y.G., 2002. Evolution of microstructure and properties of phenolic resin-based carbon/carbon composites during pyrolysis. *Materials Chemistry and Physics*, 73(2-3), pp.162-169.
- Uriarte, A.K., 2000. Nitrous oxide (N<sub>2</sub>O)—Waste to value. In *Studies in Surface Science and Catalysis* (Vol. 130, pp. 743-748). Elsevier.

USIC, 2019-last update, Inflation Calculator. Available: <https://www.usinflationcalculator.com> [May 16, 2019].

Vol'-Epshtein, A.B., Gagarin, S.G., 1973, *Kataliticheskie prevrashcheniya alkilfenolov [Catalytic conversion of alkylphenols]* [In Russian]

Wallace, J. and Updated by Staff, 2000. Phenol. *Kirk-Othmer encyclopedia of chemical technology*.

Wang, S., Adanur, S. and Jang, B.Z., 1997. Mechanical and thermo-mechanical failure mechanism analysis of fiber/filler reinforced phenolic matrix composites. *Composites Part B: Engineering*, 28(3), pp.215-231.

Weast, R.C., Astle, M.J. and Beyer, W.H., 1988. *CRC handbook of chemistry and physics* (Vol. 69). Boca Raton, FL: CRC press.

Yang, J. and Black, J.R., Shell Oil Co, 2006. *Process for producing phenol and ketone using neutralizing base*. U.S. Patent 7,141,703.

Yang, J.H., Sun, G., Gao, Y., Zhao, H., Tang, P., Tan, J., Lu, A.H. and Ma, D., 2013. Direct catalytic oxidation of benzene to phenol over metal-free graphene-based catalyst. *Energy & Environmental Science*, 6(3), pp.793-798.

Zakoshansky, V.M., 2009. Alternative technologies for the producing phenol. *Russian Journal of General Chemistry*, 79(6).

Zakoshansky, V.M., 2007. The cumene process for phenol-acetone production. *Petroleum Chemistry*, 47(4), pp.273-284.

Zárate, C.N., Aranguren, M.I. and Reboredo, M.M., 2008. Thermal degradation of a phenolic resin, vegetable fibers, and derived composites. *Journal of applied polymer science*, 107(5), pp.2977-2985.

## APPENDICES

### Appendix I Calculation of valve tray

Parameters for calculation were taken from Aspen Hysys Specifications, they can be found in Table XXIV. An example of valve tray calculation by Eq. 16-46 for column D-8 is described below (Timonin 2002, Industry standard 1983).

Table XXIV Parameters for tray calculation for column D-8

Column	D-8
Fluid load L, kg/s	2.6
Steam load G, kg/s	2.5
Liquid density $\rho_L$ , kg/m <sup>3</sup>	736.4
Vapor density $\rho_V$ , kg/m <sup>3</sup>	4.0
Surface tension $\sigma$ , mN/m	14.7

$$K_2 = 0.549 \cdot \sigma^{0.2} \quad (16)$$

where  $K_2$  is surface tension dependent coefficient,  $\sigma$  is surface tension.

$$K_2 = 0.549 \cdot 14.7^{0.2} = 0.94$$

$$A_1 = \sqrt{\frac{\rho_L - \rho_V}{\rho_L}} \quad (17)$$

where  $A_1$  is first calculated coefficient,  $\rho_L$  is liquid density,  $\rho_V$  is vapor density.

$$A_1 = \sqrt{\frac{736.4 - 4}{736.4}} = 13.5$$

$$A_2 = \frac{L}{G} \cdot \sqrt{\frac{\rho_V}{\rho_L}} \quad (18)$$

where  $A_2$  is second calculated coefficient, L is fluid load, G is steam load.

$$A_2 = \frac{2.6}{2.5} \cdot \sqrt{\frac{4}{736.4}} = 0.077$$

$$G_V = \frac{G}{\rho_V} \quad (19)$$

where  $G_V$  is steam volume load.

$$G_V = \frac{2.5}{4} = 0.62 \text{ m}^3/\text{s}$$

$$L_V = \frac{L}{\rho_L} \quad (20)$$

where  $L_V$  is fluid volume load.

$$L_V = \frac{2.6}{736.4} = 0.0035 \text{ m}^3/\text{s}$$

$$W_{pc} = 0.1 \cdot A_1 \quad (21)$$

where  $W_{pc}$  is permissible steam velocity in the column.

$$W_{pc} = 0.1 \cdot 13.5 = 1.35 \text{ m/s}$$

$$D_c = \sqrt{\frac{1.274 \cdot G_V}{W_p}} \quad (22)$$

where  $D_c$  is calculated tray diameter.

$$D_c = \sqrt{\frac{1.274 \cdot 0.62}{1.35}} = 0.77 \text{ m}$$

Standard tray diameter is selected based on calculated diameter at this step. The diameter of 1.8 m was chosen because smaller diameters exceeded permissible hydraulic resistance.

$$S = 0.785 \cdot D^2 \quad (23)$$

where  $S$  is column free cross-section,  $D$  is tray diameter.

$$S = 0.785 \cdot 1.8^2 = 2.5 \text{ m}^2$$

$$W = \frac{G_V}{S} \quad (24)$$

where  $W$  is steam velocity.

$$W = \frac{0.62}{2.5} = 0.25 \text{ m/s}$$

$$F = W \cdot \sqrt{\rho_V} \quad (25)$$

where  $F$  is steam load factor.

$$F = 0.25 \cdot \sqrt{4} = 0.49 \frac{\text{kg}^{0.5}}{\text{m}^{0.5}\text{s}}$$

Overflow edge perimeter  $l_2 = 1.04$  and overflow relative free cross-section  $S_2 = 4.51$  were selected based on tray diameter.

$$S_1 = 1 - 0.02 \cdot S_2 \quad (26)$$

where  $S_1$  is column working relative free cross-section,  $S_2$  is overflow relative free cross-section.

$$S_1 = 1 - 0.02 \cdot 4.51 = 0.91$$

$$L_{V1} = \frac{L_V}{S \cdot S_1} \quad (27)$$

where  $L_{V1}$  is fluid load per unit tray density.

$$L_{V1} = \frac{0.0035}{2.5 \cdot 0.91} = 0.0015 \text{ m/s}$$

Load factor  $B_1 = 0.086$  was selected based on value of  $A_1$ .

$$\begin{aligned} B_1 &= 0.086 \\ W_p &= K_2 \cdot B_1 \cdot A_1 \end{aligned} \quad (28)$$

where  $W_p$  is permissible steam velocity in tray working cross-section.

$$\begin{aligned} W_p &= 0.94 \cdot 0.086 \cdot 13.5 = 1.1 \text{ m/s} \\ L_{V2} &= \frac{L_V}{l_2} \end{aligned} \quad (29)$$

where  $L_{V2}$  is fluid load per unit of overflow edge perimeter length,  $l_2$  is overflow edge perimeter.

$$L_{V2} = \frac{0.0035}{1.04} = 0.0035 \text{ m/s}$$

Tray with a gear overflow plate is accepted because  $L_{V2} < 0.017 \text{ m/s}$ .

$$h_1 = 1.44 \cdot L_{V2}^{\frac{2}{3}} \quad (30)$$

where  $h_1$  is backwater height above overflow edge.

$$\begin{aligned} h_1 &= 1.44 \cdot 0.0035^{\frac{2}{3}} = 0.03 \text{ m} \\ h_5 &= h_9 = 0.05 \text{ m} \end{aligned}$$

Minimum bubbling depth  $h_5 = 0.05 \text{ m}$  and initial bubbling depth  $h_9 = 0.05 \text{ m}$  were selected.

$$h_2 = h_5 \cdot \frac{1000}{\rho_L} \quad (31)$$

where  $h_2$  is height of gas-liquid layer on tray.

$$\begin{aligned} h_2 &= 0.05 \cdot \frac{1000}{736.4} = 0.07 \text{ m} \\ h_7 &= h_2 - h_1 \end{aligned} \quad (32)$$

where  $h_7$  is overflow edge height.

$$\begin{aligned} h_7 &= 0.07 - 0.02 = 0.05 \text{ m} \\ h_6 &= (h_7 + h_1) \cdot \frac{\rho_L}{1000} \end{aligned} \quad (33)$$

where  $h_6$  is dynamic bubbling depth.

$$\begin{aligned} h_6 &= (0.05 + 0.02) \cdot \frac{736.4}{1000} = 0.05 \text{ m} \\ W_{kmin} &= 1.44 \cdot h_7^{0.35} \cdot L_{V1}^{0.3} \sqrt{\frac{\rho_L}{\rho_V}} \end{aligned} \quad (34)$$

where  $W_{kmin}$  is minimum steam velocity in free cross-section of valves.

$$W_{kmin} = 1.44 \cdot 0,05^{0,35} \cdot 0.0015^{0,3} \sqrt{\frac{736.4}{4}} = 0.64 \text{ m/s}$$

Based on tray diameter standard relative tray free cross-section  $f_3 = 12 \%$  and standard valve count  $KL=232$  were selected. Load reduction coefficient  $K_3 = 0.5$ .

$$K_1 = \frac{K_3 \cdot W \cdot 100}{f_3 \cdot W_{kmin}} \quad (35)$$

where  $K_1$  is phase equilibrium coefficient,  $K_3$  is load reduction coefficient,  $f_3$  is relative tray free cross-section

$$K_1 = \frac{1 \cdot 0.3 \cdot 100}{12 \cdot 0.64} = 1.6$$

Working relative tray free cross-section  $f_5 = f_3 = 12 \%$  because  $K_1 \geq 1$ .

$$W_k = \frac{100 \cdot W}{f_5} \quad (36)$$

where  $W_k$  is steam velocity in free cross-section of valves,  $f_5$  is working relative tray free cross-section.

$$W_k = \frac{100 \cdot 0.25}{12} = 2.05 \text{ m/s}$$

Open valve hydraulic resistance coefficient  $\zeta_o = 4.7$ , coefficient of hydraulic resistance technological valve gaps  $\zeta_h = 215$ , specific valve load  $q = 156.6 \text{ Pa}$ .

$$W_{kmax} = W_{kmin} \sqrt{\frac{\zeta_h}{\zeta_o}} \quad (37)$$

where  $W_{kmax}$  is maximum steam velocity in free cross-section of valves,  $\zeta_o$  is open valve hydraulic resistance coefficient,  $\zeta_h$  is coefficient of hydraulic resistance technological valve gaps.

$$W_{kmax} = 0.64 \cdot \sqrt{\frac{215}{4.7}} = 4.33 \text{ m/s}$$

$$F_{kmax} = W_{kmax} \cdot \sqrt{\rho_V} \quad (38)$$

where  $F_{kmax}$  is maximum steam load factor.

$$F_{kmax} = 4.33 \cdot \sqrt{4} = 8.7 \frac{\text{kg}^{0,5}}{\text{m}^{0,5}\text{s}}$$

$$A_3 = \frac{2 \cdot q}{W_k^2 \cdot \rho_V} - 0.82 \quad (39)$$

where  $A_3$  is third calculated coefficient,  $q$  is specific valve load.

$$A_3 = \frac{2 \cdot 156.6}{2.05^2 \cdot 4} - 0.82 = 17.9$$

Valve opening coefficient  $B_3$  was calculated because  $A_3 > 0$ .

$$B_3 = \frac{1.5}{\sqrt{A_3}} \quad (40)$$

where  $B_3$  is valve opening coefficient.

$$B_3 = \frac{1.5}{\sqrt{17.9}} = 0.35$$

$$\beta = -\frac{0.1}{\frac{30 \cdot W}{f_5} + 4} + \frac{0.2529}{\sqrt{h_6}} \quad (41)$$

where  $\beta$  is ailing factor.

$$\beta = -\frac{0.1}{\frac{30 \cdot 0.25}{12} + 4} + \frac{0.2529}{\sqrt{0.05}} = 0.57$$

$$p_{hr} = 5000 \cdot \zeta_k \cdot \left(\frac{F}{f_5}\right)^2 + 9810 \cdot \beta \cdot h_6 \quad (42)$$

where  $p_{hr}$  is hydraulic resistance.

$$p_{hr} = 5000 \cdot 4.7 \cdot \left(\frac{0.49}{12}\right)^2 + 9810 \cdot 0.57 \cdot 0.05 = 388.5 \text{ Pa}$$

Hydraulic resistance  $p_{hr} < 450 \text{ Pa}$ , that is why calculation can be continued. Distance between trays  $H = 0.5 \text{ m}$ , foaming coefficient  $K_5 = 0.8$ .

$$H_c = H - \frac{2.5 \cdot h_6}{K_5} \quad (43)$$

where  $H_c$  is height of separational space,  $H$  is distance between trays.

$$H_c = 0.5 - \frac{2.5 \cdot 0.05}{0.8} = 0.4 \text{ m}$$

$$e = \frac{5.7 \cdot 10^{-3}}{O} \cdot \left(\frac{W}{H_c}\right)^{3.2} \quad (44)$$

where  $e$  is liquid entrainment between trays.

$$e = \frac{5.7 \cdot 10^{-3}}{14.7} \cdot \left(\frac{0.25}{0.4}\right)^{3.2} = 8.7 \cdot 10^{-5}$$

$$U = \frac{L_V \cdot 100}{S \cdot S_2} \quad (45)$$

where  $U$  is fluid velocity in overflow.

$$U = \frac{0.0035 \cdot 100}{2.5 \cdot 4.51} = 0.031 \text{ m/s}$$

$$U_p = 0.008 \cdot K_5 \cdot \sqrt{H \cdot (\rho_L - \rho_V)} \quad (46)$$

where  $U_p$  is permissible fluid velocity in overflow,  $K_5$  is foaming coefficient.

$$U_p = 0.008 \cdot 0.8 \cdot \sqrt{0.5 \cdot (736.4 - 4)} = 0.12 \text{ m/s}$$

The fluid velocity in overflow is below the permissible, it means that the calculated tray can be used. The calculation of the valve tray diameter is over.

## Appendix II Calculation of vessel mass

Volume of vessel steel and its density is required for vessel mass calculation. The height of the column is calculated by multiplying the distance between the trays by the number of real trays. Energy conversion efficiency is used to convert theoretical stages into number of real trays. An example of the column D-8 height calculation is described below. Energy conversion efficiency  $\eta_{valve} = 0.8$  for valve tray (Couper, Penney et al. 2012).

$$n_{real} = \frac{n_t}{\eta_{valve}} \quad (47)$$

where  $n_{real}$  is number of real trays,  $n_t$  is theoretical number of stages,  $\eta_{valve}$  is energy conversion efficiency for valve tray.

$$n_{real} = \frac{40}{0.8} = 50$$

$$H_v = H \cdot n_{real} \quad (48)$$

where  $H_v$  is vessel height,  $H$  is distance between trays.

$$H_v = 0.5 \cdot 50 = 25 \text{ m}$$

It was decided to use stainless steel because of corrosion by components (Revie 2011).

Column D-8 operates under atmospheric pressure ( $p = 0.1 \text{ MPa}$ ). The density is  $865 \text{ kg/m}^3$ . The height of the column is 25 m, the diameter is 1.8 m. An example of calculation of vessel mass for column D-8 is described below (Timonin 2002).

It is necessary to clarify whether hydrostatic pressure should be considered.

$$p_h = \rho \cdot g \cdot H_v \quad (49)$$

where  $p_h$  is hydraulic pressure,  $\rho$  is density,  $g$  is gravitational acceleration between trays.

$$p_h = 865 \cdot 9.81 \cdot 25 = 0.21 \text{ MPa}$$

$$\frac{p_h}{p} = \frac{0.21}{0.1} \cdot 100 \% = 210 \%$$

Since the hydrostatic pressure is more than 5 %, it must be considered. Calculated pressure:

$$p_c = 0.21 + 0.1 = 0.31 \text{ MPa}$$

Test pressure is determined by Eq. 50 for vessels with pressure less than 0.5 MPa. Admissible stress for stainless steel  $\sigma_{20} = 300 \text{ MPa}$ , admissible stress for working temperature of  $160 \text{ }^\circ\text{C}$   $\sigma = 247 \text{ MPa}$  (Sassda 2017). Weld strength factor  $\varphi = 1$ .

$$p_t = 1.5 \cdot p_c \cdot \frac{\sigma_{20}}{\sigma} \quad (50)$$

where  $p_t$  is test pressure,  $p_c$  is calculated pressure,  $\sigma_{20}$  is admissible stress for 20 °C,  $\sigma$  is admissible stress for working temperature.

$$p_t = 1.5 \cdot 0.31 \cdot \frac{300}{257} = 0.54 \text{ MPa}$$

$$s = s_c + c \quad (51)$$

where  $s$  is wall thickness,  $s_c$  is calculated wall thickness,  $c$  is allowance.

$$s_c = \frac{p_t \cdot D_d}{2 \cdot \varphi \cdot \sigma - p_t} \quad (52)$$

where  $D_d$  is vessel diameter,  $\varphi$  is weld strength factor.

$$s_c = \frac{0.54 \cdot 1800}{2 \cdot 1 \cdot 257 - 0.54} = 1.9 \text{ mm}$$

$$c = c_1 + c_2 + c_0 \quad (53)$$

where  $c_1$  is corrosion allowance,  $c_2$  is negative tolerance allowance,  $c_0$  is standard rolled thickness allowance.

$$c_1 = J \cdot \tau \quad (54)$$

where  $J$  is corrosion ratio,  $\tau$  is life span.

$$c_1 = 0.1 \cdot 15 = 1.5 \text{ mm}$$

The nearest standard sheet thickness for calculated wall thickness with corrosion allowance is 4 mm. The negative tolerance allowance for a 4 mm thickness sheet is 0.4 mm (Pland 2015), that is why  $c_0 = 0.2 \text{ mm}$ .

$$c = 1.5 + 0.4 + 0.2 = 2.1 \text{ mm}$$

$$s = 1.9 + 2.1 = 4 \text{ mm}$$

Finally, vessel wall thickness is  $s = 4 \text{ mm}$ .

Approximate density for stainless steel is 7900 kg/m<sup>3</sup> (The Physics Factbook 2019).

$$m = \rho_{steel} \cdot V_{vessel} \quad (55)$$

where  $m$  is vessel mas,  $\rho_{steel}$  is steel density,  $V_{vessel}$  is volume of vessel steel.

$$V_{vessel} = \frac{(\pi \cdot D_e^2)}{4} \cdot H_v - \frac{(\pi \cdot D_i^2)}{4} \cdot H_v + 2 \cdot \left( \frac{4\pi \cdot \left(\frac{D_e}{2}\right)^3}{3} - \frac{4\pi \cdot \left(\frac{D_i}{2}\right)^3}{3} \right) \quad (56)$$

where  $D_e$  is external diameter,  $D_i$  is internal diameter.

$$V_{vessel} = \frac{(\pi \cdot 1.808^2)}{4} \cdot 25 - \frac{(\pi \cdot 1.8^2)}{4} \cdot 25 + 2 \cdot \left( \frac{4 \cdot \pi \cdot \left(\frac{1.808}{2}\right)^3}{3} - \frac{4 \cdot \pi \cdot \left(\frac{1.8}{2}\right)^3}{3} \right) = 0.61 \text{ m}^3$$

$$m_2 = 7900 \cdot 1,66 = 13114 \text{ kg}$$

The calculation of the vessel mass is over.